Investigating Macro- and Micro-Scale Material Provenancing Signatures in Uranium Ore Concentrates/Yellowcake

A. Wotherspoon, L. Vance, J. Davis, J. Hester, D. Gregg, G. Griffiths, I. Karatchevtseva, Y. Zhang, T. Palmer, E. Keegan, N. Blagojevic, E. Loi, D. Hill, M. Reinhard

Australian Nuclear Science and Technology Organisation (ANSTO)
Lucas Heights, New South Wales
Australia

Abstract. Australia possesses the world's largest estimated recoverable resources of uranium bearing ore, and consequently it is of interest to ensure the safe extraction and export of this high value fungible commodity.

Currently, no singular analysis technique has been capable of elucidating the origins of all UOC materials. The Australian Nuclear Science and Technology Organisation's Nuclear Forensics Research Facility (ANSTO-NFRF) is in the process of examining diffuse reflectance spectroscopy (DRS) of yellowcake materials in the range of the near-infrared (IR) (4000-12500 cm^{-1}), and as colour is an important indicator of processing, the UV/VIS wavelengths (50000-12500 cm^{-1}) amongst other techniques. We have also examined the far-infrared in transmission mode (700-20 cm^{-1}), to distinguish between UOC of known ore/mining/extraction age containing different species and polymorphs of uranium and confirmed phases/structures with XRD and/or neutron diffraction. SEM provided substantive answers on particulate morphology. Neutron and X-ray diffraction allowed identification of minor phase differences, characteristic of material provenance/processing. Positron annihilation lifetime spectroscopy showed only quite minor differences between samples.

1. Introduction

The earliest stages of the nuclear fuel cycle involve the production of uranium ore concentrate (UOC). Presently, tracing either the source or provenance of unknown UOC is a formidable task and results in most cases to a simple narrowing of potential sources. The main efforts on 'profile' analyses comprise chemical and elemental signatures and physical characteristics. Still in its comparative infancy, Nuclear Forensics is a developing discipline, but pivotal to dealing with nuclear security events. A number of physical analysis based techniques have been applied to determine origin[1] for nuclear based materials. UOC samples by virtue of their lesser purity, have been examined by elemental and anionic impurity content [2],[3],[4],[5]. Other workers in this field have examined U, Pb, Sr isotopes [6],[7],[8] and rare earth 'profiles' [9,10]. Independently these techniques are usually not sufficiently discriminatory for positive identification. Elemental and anionic data [2] from UOC sourced from primarily Australia and Canada, suggest that statistical analysis of phosphorite and quartz-pebble conglomerate, contained a distinct impurity composition. Samples grouped according to their geographical region of origin appeared to contain distinctive impurities in certain cases (Elliott Lake and Bancroft, Ontario).

A less labour intensive analysis, based upon the Visible/Near-Infrared Reflectance Spectroscopy (VS/NIR DRS) over the range of 350-2500 nm has been used [11]. Investigations using DRS in the far-infra-red region to measure pure samples of UO_2, U_3O_8 and γ-UO_3 began as early as 1989 [12], but it is only relatively recently that the Vis/NIR region was examined [11]. In this paper we seek to further study the complementary nature of the various instrumental techniques examined to provide additional clues and further aid the elucidation of unknown yellowcake materials.

2. Samples and Experimental

Ten UOC samples from Australia were used in the course of this study. Although uranium production in Australia begun in the period from 1954-1971, we decided to examine only operating and exporting

second generation mines (1976 to present), *viz*. Beverley, Ranger, and Olympic Dam (O.D.).

Table 1: Australian uranium ore concentrate samples analysed for uranium speciation and microstructural features[2].

Mine/mill (sample name)	Region or State	Period of operation	Deposit Type	Primary U minerals	Gangue Minerals	Processing
Olympic Dam	South Australia	1988-	Hematite/breccia complex	Uraninite, coffinite brannerite	Iron oxides, Chlorite, sericite, clay minerals	Complex processing (due to recovery of Cu, U, Ag, and Au). H_2SO_4 leach, SX, $(NH_4)_2SO_4$ strip, NH_3 pptn of U
Ranger	Northern Territory	1980-	Unconformity related	Uraninite, brannerite, pitchblende	Refractory gangue, chlorite Muscovite, Clay minerals	H_2SO_4 leach, SX, $(NH_4)_2SO_4$ strip, NH_3 pptn of U
Beverley	South Australia	2001-	Sandstone Basal/Palaeochannel	Coffinite, uraninite	Quartz, clay, feldspar, traces of gypsum	H_2SO_4 leach/H_2O_2, IX, washed with salt/dil. H_2SO_4, neutralized NaOH(aq), pptn with H_2O_2

IX=ion exchange, SX=solvent extraction, pptn=precipitation.

The samples ranged in colour from dark yellow (Beverley, $UO_4.nH_2O$) to dark green/black (U_3O_8, Ranger and Olympic Dam) respectively. Colour is indicative of calcination temperature.

2.1. Experimental

2.1.1. Scanning Electron Microscopy (SEM)

The powdered material was dropped onto a double sided conductive carbon adhesive tape and approximately 50 Å of platinum was evaporated onto the surface under vacuum to prevent charging during SEM examination. The SEM used was a JEOL JSM-6300 SEM operated at 15 keV. The instrument is housed in a dedicated active characterization laboratory for handling radioactive samples. The powdered material was also mounted in an epoxy resin and polished to a 1-micron diamond finish. Approximately 50 Å of carbon was evaporated onto the surfaces under vacuum to prevent charging. These epoxy mounted samples were then analysed with a Zeiss Ultra Plus SEM operated at an accelerating voltage of 15 kV.

2.1.2. VIS/NIR Spectroscopy

Diffuse reflectance (DR) spectra over the range of 350-2500 nm were measured on pressed pellets at ambient temperature using a Cary 5000 spectrophotometer (Agilent, Palo Alto, CA) equipped with a Labsphere Biconical Accessory. Spectra are referenced to that of a Labsphere certified standard (Spectralon), and transformed into absorption units. Samples were analyzed as pellets as received.

2.1.3. X-ray Diffraction (XRD)

Chemical phase information was obtained through XRD pattern matching using the X'Pert Highscore package (Panalytical, Spectris, UK) and the 2009 database from the International Centre for Diffraction Data (ICDD). Powder XRD patterns were collected on all yellowcake samples on a Panalytical powder diffractometer. The diffractometer uses a Cu Kα graphite monochromated source and is outfitted with a D/Tex silicon strip detector. Typically, the collection of the XRD patterns took 6 hours per material.

2.1.4. Neutron Diffraction

We used neutron diffraction as a complementary technique due to the higher relative sensitivity of neutrons to light atoms in the presence of U when compared with XRD. This would expose otherwise invisible differences in the samples, notably diffuse scattering from hydrogenous material.

Neutron diffraction patterns were collected on the Echidna High Resolution Powder Diffractometer at the OPAL reactor, ANSTO, Australia (Liss *et.al*.) [13] at a wavelength of 1.62A with 10' pre-sample collimation. One pattern required 6h to acquire.

2.1.5. Transmission IR

Far-infrared spectroscopy (Far-IR) spectra were obtained on a Nicolet Nexus 8700 FTIR spectrometer (Thermo Electron Corporation, Madison, WI) using the DTGS PE detector. Spectra were collected in transmission mode from 150 to 700 cm^{-1} range by averaging 1024 scans with 4 cm^{-1} resolution. Powders were diluted with dried CsI and pressed into pellets.

2.1.6. Positron Annihilation Lifetime Spectroscopy (PALS)

Positron annihilation lifetime spectroscopy (PALS) is a non-destructive spectroscopy technique to study voids and defects in solids. [2] The source of the positrons is sodium-22. This annihilation releases gamma rays that can be detected; the time between emission of positrons from a radioactive source and detection of gamma rays due to annihilation of positrons with electrons corresponds to the lifetime of the positron. For solids containing free electrons (such as metals or semiconductors), the implanted positrons annihilate rapidly unless voids such as vacancy defects are present. If voids are available, positrons will reside in them and annihilate less rapidly than in the bulk of the material, on time scales up to ~several ns, depending on the void geometry.

The PALS apparatus was a fast-fast coincidence spectrometer, with scintillation detectors based on Hamamatsu H3378-51 (25SE25) photomultiplier tubes and BaF_2 scintillators (Nucletron, Newton, NSW2042, Australia). A 1.1 MBq $^{22}NaCl$ source was used for collecting spectra; the source was encapsulated in 8 μm Kapton foil. Experiments were carried out in a sandwich geometry between two identical samples. The time resolution of the instrument was determined to be 265 ps from the FWHM of a ^{60}Co prompt peak under actual experimental conditions.

3. Results and Discussion

3.1. SEM

The SEM results for three mines are presented in Fig. 1 and 2 for particulate and polished epoxy mounted particulate respectively.

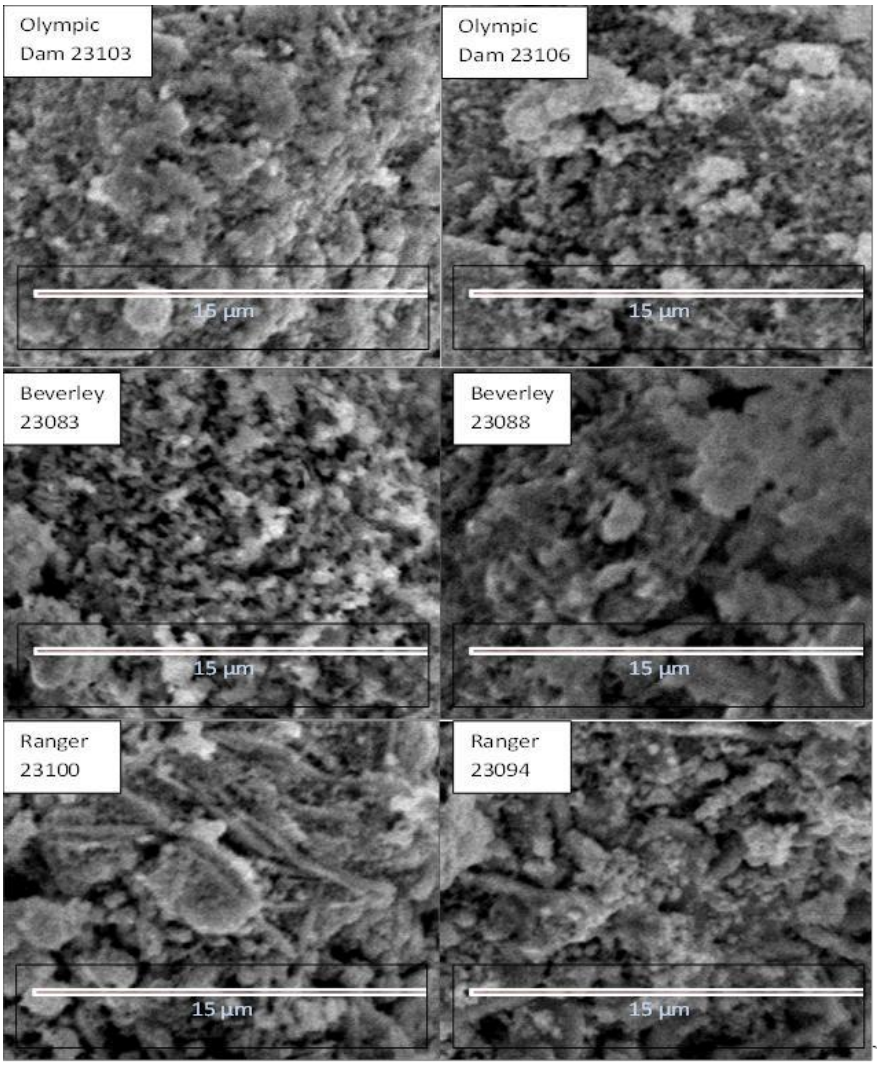

Fig.1: SEM for intact particulate yellowcake samples coated with platinum. All magnifications X 1500.

Figs.1 and 2 illustrate the different structures of intact and polished UOC materials respectively at 1,500 X magnification. All particulates in the main have similar sizes (~100 µm) and are almost spherical in shape; however intrinsic surface morphological differences could be observed. Examining both U_3O_8 containing materials, one can see that both Ranger and O.D. have large particle sizes with surficial adherence of smaller particles of approximately 1/8th the diameter of the parent. O.D. presented a much smoother surface for the large particles, quite unlike Ranger material which had rod-like protrusions. Beverley, the sole uranium peroxide hydrate, also presented a roughened surface with the appearance of scale-like features. In all cases, cutting and polishing through the particles and examination at 1,500 X more clearly illustrated the gross internal micro-structural features, and in particular the crystalline rod structure present in the Ranger UOC.

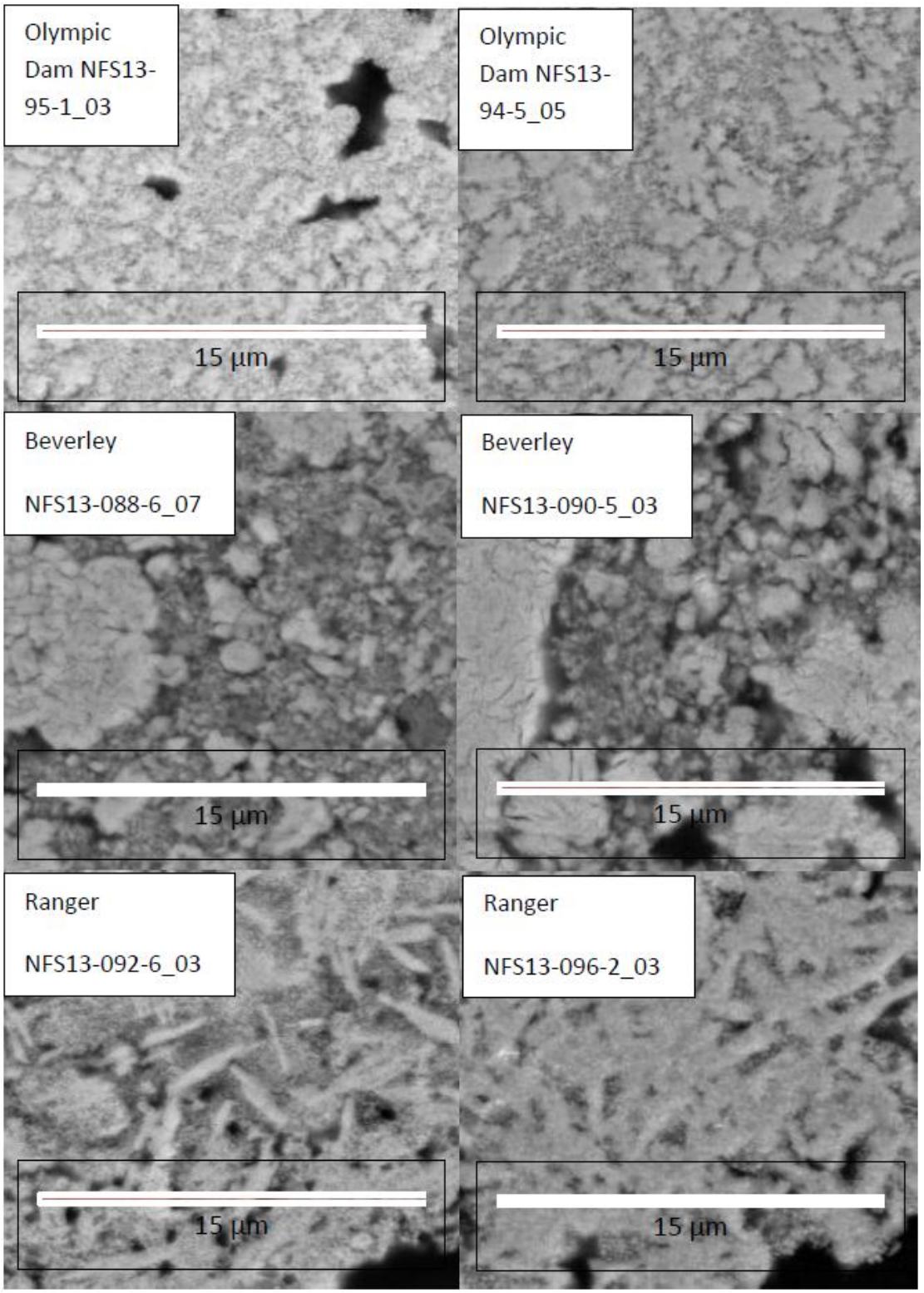

Fig.2: SEM Epoxy mounted, polished, carbon coated, yellowcake samples.

3.2. Diffuse Reflectance Spectrometry/Transmission IR

DRS in NIR has been recently shown to be a particularly useful non-destructive technique for identifying the speciation, notably the valence, of uranium. This was demonstrated herein, with Figs. 3 and 4 showing major differences in the absorption of the two U_3O_8 samples *vs* the $UO_4.nH_2O$. Subtle differences in the absorption peaks were observed between the two U_3O_8 exporting mines (Fig. 4, ~1500 and 1860 nm) will be examined further to determine the consistency for multivariate Discrimination for this uranium oxide from these two mines.

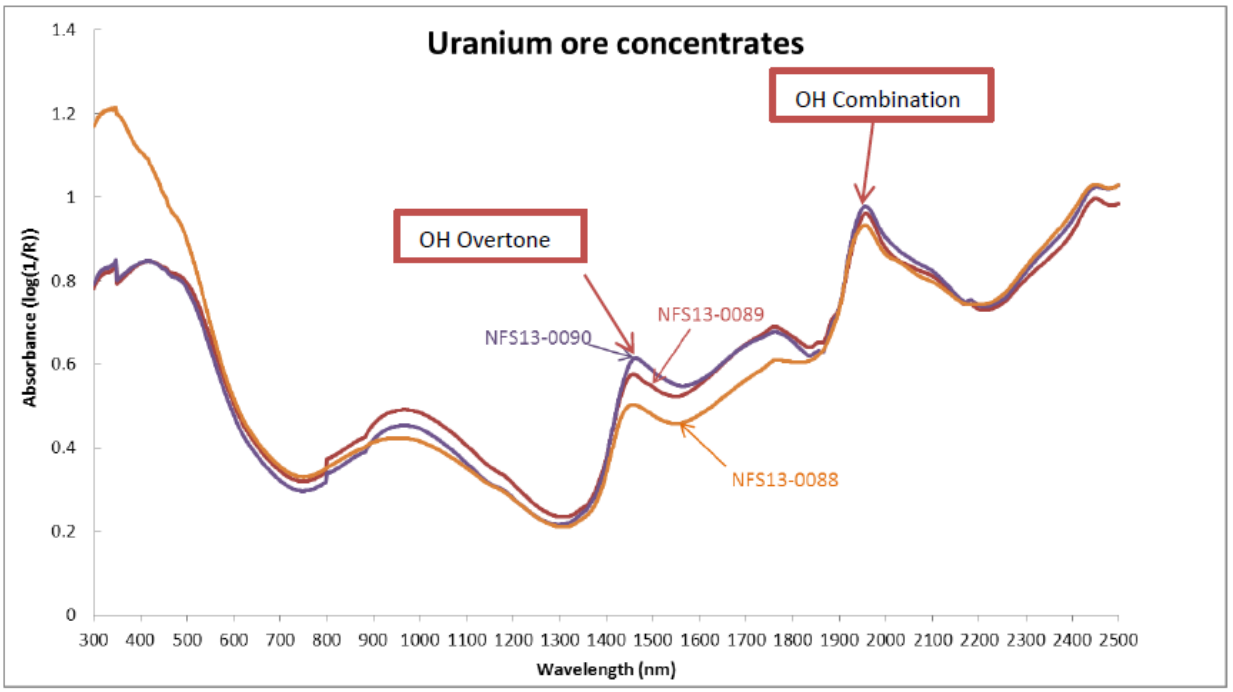

Fig.3: Full scan Vis/NIR spectra of Beverly UOCs ($UO_4.nH_2O$).

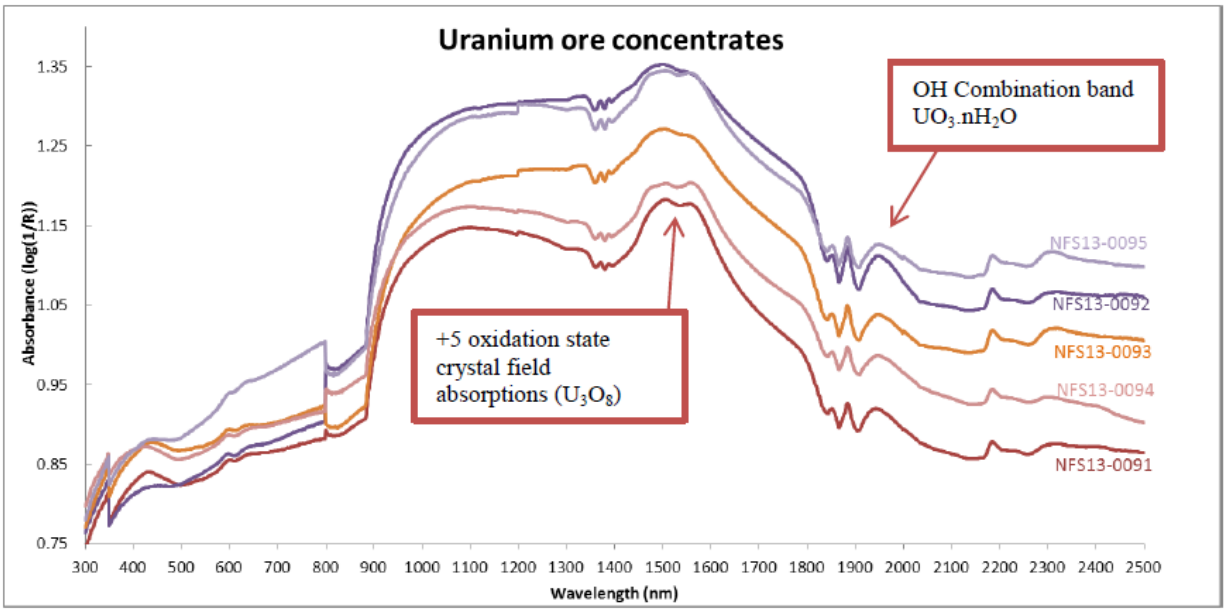

Fig.4: Full scan Vis/NIR spectra of Olympic Dam (NFS13-0094+0095) and Ranger (NFS13-0091 to NFS13-0093) UOCs (U_3O_8). Note grating changes at ~350 and 780 nm in both Figures 3 and 4.

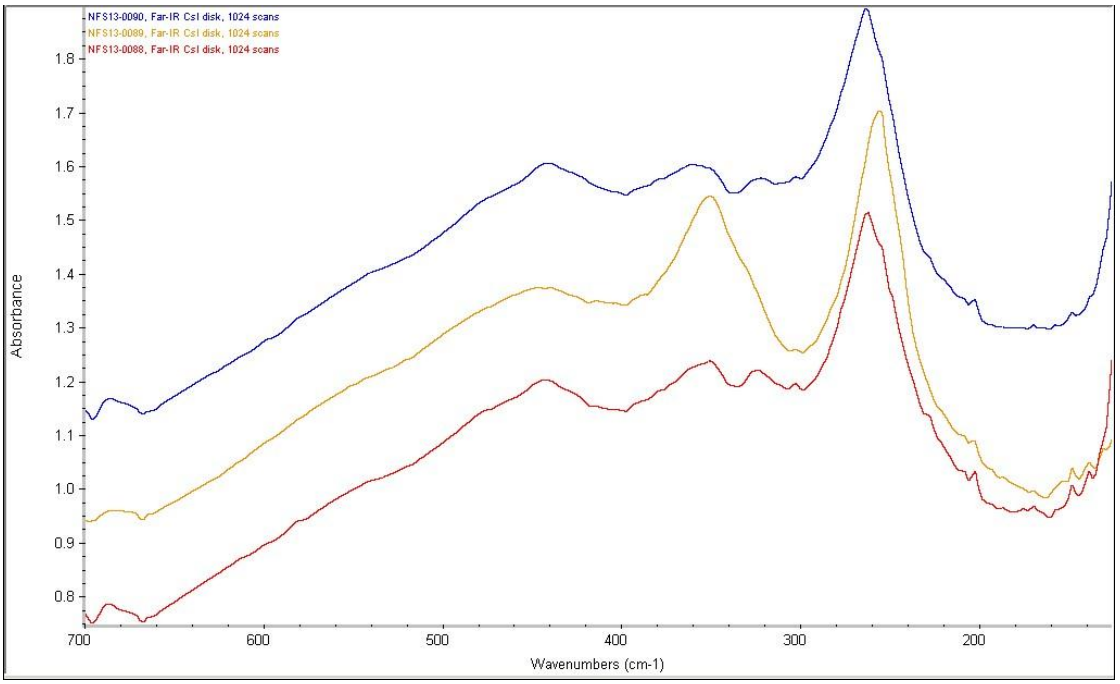

Fig. 5.: Transmission mode Far IR of Beverley UOC (CsI disk)

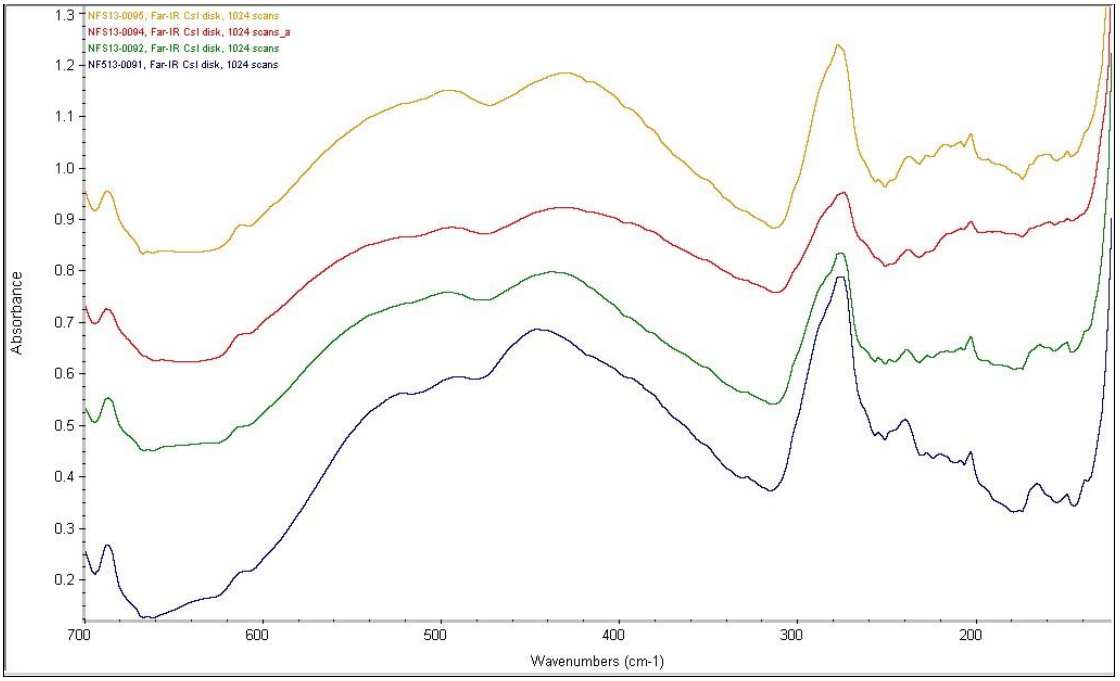

Fig. 6.: Transmission mode Far IR of Olympic Dam (NFS13-0094+0095) and Ranger UOC (NFS13-0091 to NFS13-0093) as CsI disks.

Transmission far IR also appears to be capable of identifying the speciation of uranium. This was demonstrated herein, with **Figs. 5-7** showing gross differences in the phonon absorption of the two U_3O_8 samples *vs* the $UO_4.nH_2O$. Samples from the two U_3O_8 mines (**Fig. 6**) will be analysed numerous times to determine the consistency for multivariate discrimination to aid identification. However, as these spectra have weak peaks due to lattice mode vibrations, they may be of limited usefulness in identifying subtle differences in common speciation from mines producing the same UOC type.

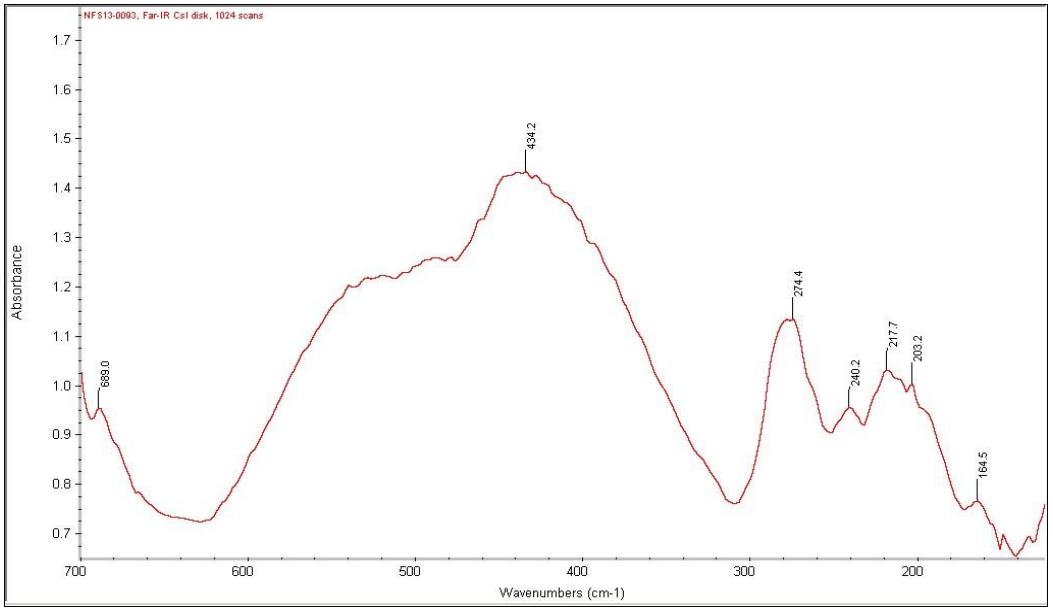

Fig.7: Transmission mode Far IR of Ranger UOC (CsI disk)

3.3. X-Ray and Neutron Diffraction (ND)

The neutron diffraction patterns confirmed the XRD phase identifications, and as expected the ND displayed high backgrounds in those samples with relatively high amounts of water, due to incoherent scattering from H atoms.

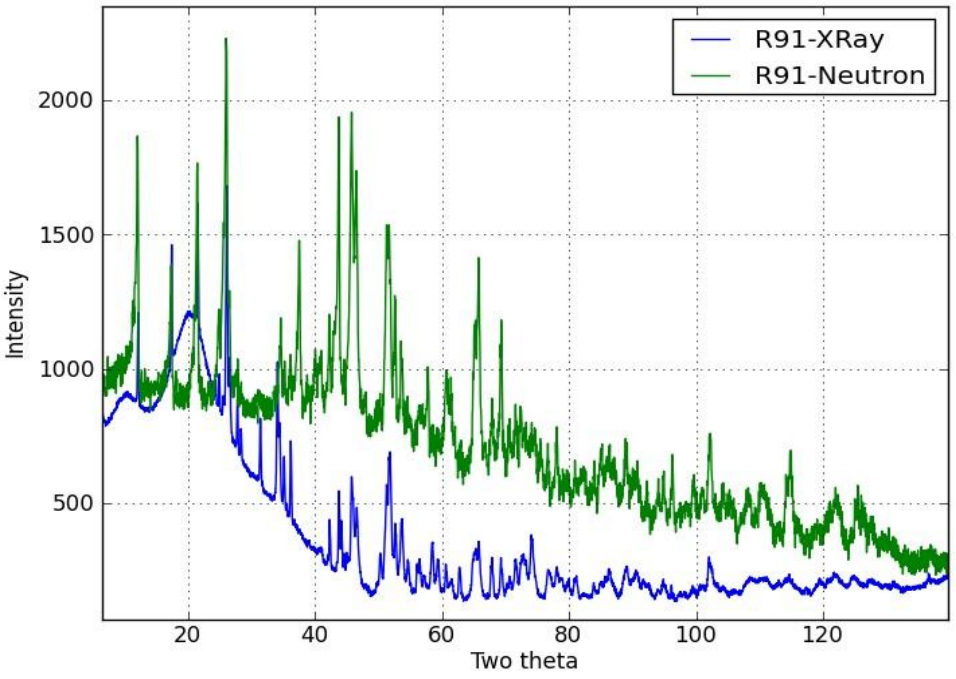

Fig. 8: Overlay of Ranger UOC X-ray and neutron patterns normalised to the same λ (Cu Kα)

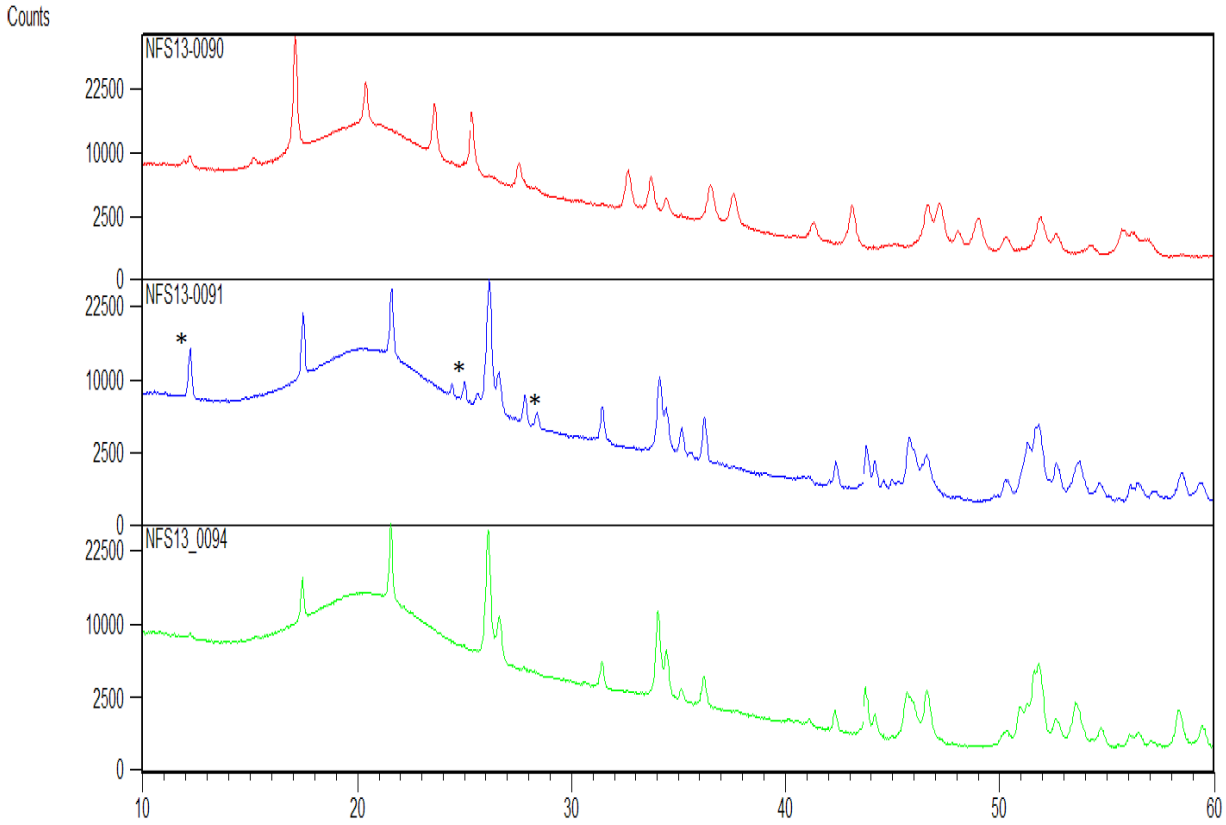

Fig. 9: XRD patterns of respectively Beverley (upper trace in red), Ranger middle trace in blue, and Olympic Dam mine UOC Samples. Distinguishing lines differentiating Ranger from OD are indicated as shown*. Diffuse scattering due to sample holder is evident from 2θ=13-26˚.

XRD is routinely used for phase determination and quantification in industrial settings. Following standard phase identification procedures and with comparisons to published ICDD data, the Ranger sample is predominantly U_3O_8 and $UO_3.2H_2O$, whilst Olympic Dam is predominantly U_3O_8 and trace $UO_3.2H_2O$[13]. The Beverley sample, which is exported as uranium peroxide, does contain a majority of $UO_4.2H_2O$ and trace $UO_4.4H_2O$ and $UO_3.2H_2O$[14].

3.4. PALS

The PALS results (Table II) on all four samples examined were very similar, so the potential of PALS for discrimination at this stage is not strong. However we have several more samples for study at a later stage. The very weak second lifetime component is not understood as yet, but maybe due to surface effects from the different powders or grain boundary effects.

Table II: Positron Annihilation Lifetime Spectroscopy (PALS) of Selected UOCs

Sample ID	Intensity T1/T2	Ave.T1 Lifetime	Ave.T2 Lifetime (N=2)
Ranger 1	95.6/4.4	0.32	1.6
Olympic Dam 1	97.9/2.2	0.31	1.1
Beverley 2	95.0/5.0	0.34	1.7
Beverley 1	98.8/1.2	0.34	1.6

4. Conclusion

The results from a collection of experimental techniques have gone a long way in differentiating properties of yellowcake samples from different sources. We suggest IR in both DRS and transmission mode operation are useful non-destructive techniques for identifying the speciation of the yellowcake, but may not have sufficient discriminating power to infer the origin of the two U_3O_8 producing mines (Ranger and O.D.). SEM morphology discriminates between all three mines, with different structural features evident in material from all three mines. The SEM morphology of Ranger, which has the presence of crystalline rod-like structures, is suggested to contain significantly higher $UO_3.2H_20$ in comparison to O.D (**Fig.9**, additional peaks). In future work we will endeavour to clarify the identity of these rod-like protuberances in Ranger material and perform slow scanning of the UV/VIS/NIR region in DRS mode and by transmission far IR regions. We will attempt to confirm if subtle spectral features can be used to further differentiate U_3O_8 from Ranger and Olympic Dam mines. Differences in U_3O_8 and $UO_4.nH_2O$ samples in PALS maybe minimal, but more samples are available for study.

REFERENCES

[1] MAYER K, WALLENIUS M, RAY I (2005) Nuclear Forensics - A Methodology Providing Clues On The Origin Of Illicitly Trafficked Nuclear Materials. Analyst **130** (4):433-441. DOI:DOI 10.1039/B412922A

[2] KEEGAN E, WALLENIUS M, MAYER K, VARGA Z, RASMUSSEN G (2012) Attribution Of Uranium Ore Concentrates Using Elemental And Anionic Data. Applied Geochemistry **27** (8):1600-1609. DOI:10.1016/J.APGEOCHEM.2012.05.009

[3] KEEGAN E, RICHTER S, KELLY I, WONG H, GADD P, KUEHN H, ALONSO-MUNOZ A (2008) The Provenance Of Australian Uranium Ore Concentrates By Elemental And Isotopic Analysis. Applied Geochemistry **23** (4):765-777. DOI:10.1016/J.APGEOCHEM.2007.12.004

[4] SVEDKAUSKAITE-LEGORE J, RASMUSSEN G, ABOUSAHL S, VAN BELLE P (2008) Investigation Of Th Sample Characteristics Needed For The Determination Of The Origin Of Uranium-Bearing Materials. Journal Of Radioanalytical And Nuclear Chemistry **278** (1):201-209. DOI:DOI 10.1007/S10967-007-7215-Y

[5] BADAUT V, WALLENIUS M, MAYER K (2009) Anion Analysis In Uranium Ore Concentrates By Ion Chromatography. Journal Of Radioanalytical And Nuclear Chemistry **280** (1):57-61. DOI:10.1007/S10967-008-7404-3

[6] SVEDKAUSKAITE-LEGORE J, MAYER K, MILLET S, NICHOLL A, RASMUSSEN G, BALTRUNAS D (2007) Investigation Of The Isotopic Composition Of Lead And Of Trace Elements Concentrations In Natural Uranium Materials As A Signature In Nuclear Forensics. Radiochimica Acta **95** (10):601-605. DOI:DOI 10.1524/RACT.2007.95.10.601

[7] RICHTER S, ALONSO-MUNOZ A, EYKENS R, JACOBSSON U, KUEHN H, VERBRUGGEN A, AREGBE Y, WELLUM R, KEEGAN E (2008) The Isotopic Composition Of Natural Uranium Samples - Measurements Using The New N(U-233)/N(U-236) Double Spike IRMM-3636. Int J Mass Spectrom **269** (1-2):145-148. DOI:DOI 10.1016/J.IJMS.2007.09.012

[8] VARGA Z, WALLENIUS M, MAYER K, KEEGAN E, MILLETT S (2009) Application Of Lead And Strontium Isotope Ratio Measurements For The Origin Assessment Of Uranium Ore Concentrates. Analytical Chemistry **81** (20):8327-8334.

DOI:10.1021/AC901100E

[9] VARGA Z, WALLENIUS M, MAYER K (2010) Origin Assessment Of Uranium Ore Concentrates Based On Their Rare-Earth Elemental Impurity Pattern. Radiochimica Acta **98** (12):771-778. DOI:10.1524/RACT.2010.1777

[10] VARGA Z, KATONA R, STEFANKA Z, WALLENIUS M, MAYER K, NICHOLL A (2010) Determination Of Rare-Earth Elements In Uranium-Bearing Materials By Inductively Coupled Plasma Mass Spectrometry. Talanta **80** (5):1744-1749. DOI:10.1016/J.TALANTA.2009.10.018

[11] KLUNDER GL, PLAUE JW, SPACKMAN PE, GRANT PM, LINDVALL RE, HUTCHEON ID (2013) Application Of Visible/Near-Infrared Reflectance Spectroscopy To Uranium Ore Concentrates For Nuclear Forensic Analysis And Attribution. Appl Spectrosc **67** (9):1049-1056

[12] YU BZ, HANSEN WN, WARD J (1989) The Far-Infrared Spectra Of UO2, Alpha-U_3O_8, and Gamma-UO_3 Using The Light Pipe Reflection Method. Appl Spectrosc **43** (1):113-117

[13] VOCHTEN R, DEGRAVE E, LAUWERS H (1990) Transformation Of Synthetic U3O8 Into Different Uranium Oxide Hydrates. Miner Petrol **41** (2-4):247-255. DOI:DOI 10.1007/BF01168498

[14] TAYLOR P, WOOD DD, DUCLOS AM (1992) The Early Stages Of U_3O_8 Formation On Unirradiated Candu UO_2 Fuel Oxidized In Air At 200-300-Degrees-C. Journal Of Nuclear Materials **189** (1):116-123. DOI:DOI 10.1016/0022-3115(92)90425-K

Exploring Spectroscopic and Morphological Data as New Signatures for Uranium Ore Concentrates

D. Ho Mer Lin[a,d], D. Manara[a], Z. Varga[a], L. Fongaro[a], A. Nicholl[a], M. Ernstberger[a], A. Berlizov[b], P. Lindqvist[c], T. Fanghaenel[a], K. Mayer[a]

[a] European Commission
Joint Research Centre, Institute for Transuranium Elements
P.O Box 2340, 76125
Karlsruhe, Germany

[b] International Atomic Energy Agency
Vienna International Centre
P.O. Box 100, 1400 Vienna
Austria

[c] Institute of Nuclear Waste Disposal
P.O. Box 3640, 76021 Karlsruhe, Germany

[d] DSO National Laboratories
20 Science Park Drive, 118230
Singapore

Abstract. Raman spectroscopy and morphological parameters obtained from Scanning Electron Microscopy (SEM) combined with image analysis, of uranium ore concentrates (UOCs) were studied and assessed as possible signatures for nuclear forensic applications. Raman spectra and morphological data were subsequently treated separately with principal component analysis. The complementary use of infrared and Raman data adds value to the interpretation and shed reasonable doubts regarding the true composition of UOCs such as ammonium diuranate/uranyl hydroxide that resulted from overlapping clusters in PCA analysis of 95 samples. PCA analysis of 30 parameters relating to shapes and sizes of 17 UOC samples is a potential signature for origin assessment indicative of the process.

1. Introduction

As a relatively young discipline emerging from the needs to tackle illicit trafficking [1-4], nuclear forensic science continues to develop with interest in the investigation of new signatures or fingerprints to complement or improve its existing multi-faceted analysis. *Signatures* or *fingerprints*, in this sense refer to physical, chemical, isotopic characteristics associated with the nuclear materials that could potentially identify their origin, should the material be lost and subsequently found. The eventual attribution of material can subsequently lead to legal prosecution and henceforth, the studying and understanding of nuclear materials clearly plays a pivotal role in the entire process.

Originating from the early stages of the nuclear fuel cycle, *uranium ore concentrates (UOCs)* or *yellow cakes* are intermediate products as a result of mining and milling of uranium ore. These precursors of nuclear fuel are often traded in large quantities, due to ease of access compared to enriched samples and therefore, diversions or thefts are real. Three cases involving UOCs had been

published [5-7]. What is noteworthy is the fact that these yellow cakes have different compositions depending on their processing history and it is therefore necessary to differentiate or distinguish them from each other. After uranium is leached from the ore, purification and concentration of uranium are followed and subsequently, the yellow cakes are produced by precipitation. The use of precipitating reagents such as ammonium hydroxide, hydrogen peroxide, sodium hydroxide, ammonium carbonate, magnesium hydroxide/magnesium oxide will lead to the formation of ammonium diuranate, uranyl peroxide, sodium diuranate, ammonium uranyl carbonate, uranyl hydroxide, respectively. The choice of the precipitating reagents is based on the type of ore plus economics and environment factors. After the precipitation, these powders have a characteristic pale/bright yellow, orange or light brown colour. They are further subjected to drying and calcination to remove water and volatile components [8]. At temperatures of ~450 °C, another UOC known as UO_3 with a bright orange colour is produced. Further increment in temperatures to ~700 °C will lead to the formation of a dark green/black powder of U_3O_8 [9], also known collectively as yellow cake. These UOCs are further subjected to conversion whereby UF_4 and UO_2 products are also subsequently formed. These non-UOCs are also included in this study.

In view of developing signatures of UOCs for nuclear forensics purposes in answering questions such as '**what** is the material?', '**How** it was produced?', '**Where** did it come from?', there have been numerous studies published on the applicability of analyzing various aspects associated with the yellow cakes. These includes composition of major constituents including U isotopes [10, 11], minor constituents such as Th [12], Pb [13-15], Sr [14] and S isotopes [16], trace elements [10, 13, 15, 17-19], non-volatile organics [20] and anionic impurities [19, 21, 22]. The application of $^{228}Th/^{232}Th$ to the determination of production dates of 'found' impure yellow cake has been demonstrated [5, 12]. These techniques typically require very sensitive and precise measurements and are often fulfilled with the use of inductively coupled plasma mass spectrometry (ICP-MS) or thermal ionization mass spectrometry (TIMS). More recently, there have also been reports on the use of spectroscopic techniques such as infrared (IR) spectroscopy [22], near infrared reflectance spectroscopy [23, 24] and laser-induced breakdown spectroscopy (LIBS) [25] for the measurement of UOCs for origin assessment.

In this paper, we explored the feasibility of using Raman spectroscopy as a tool for nuclear forensics application. The phenomenon of light interaction with molecules typically gives rise to certain interaction between the light and material such as absorption, reflection, elastic and inelastic scattering. Raman spectroscopy is based on the inelastic light scattering to obtain information from molecular vibrations (Fig. 1). This technique is of interest owing to its non-destructive nature, ability to measure all states of matter and solution and through containment system like glass (thus hazardous/unknown substances can be probed in a safe way). Therefore, hardly any sample preparation is needed thus rapid analysis is possible. The miniaturization of Raman spectrometers has also played a critical role leading to several field applications especially in cultural heritage [26, 27], forensic [28, 29], defence and homeland security [28, 30]. A hand-held Raman on loan from International Atomic Energy Agency (IAEA) is also featured in this paper where the usefulness/performance of this instrument is briefly highlighted.

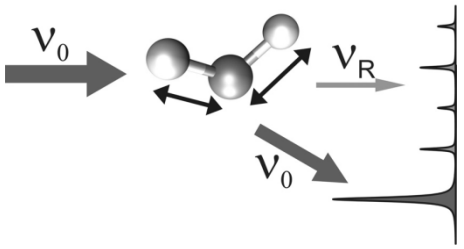

Fig. 1: Concepts of Raman scattering (v_0 being the incident laser line; v_R (thin arrow) corresponds to inelastic scattering/ the Raman lines; v_0 (thick arrow) corresponds to elastic scattering/ the Rayleigh lines [31]

A less explored signature but nonetheless an important aspect of studying uranium ore concentrates, is the correlation between their respective morphological characteristics and the processing or production history. In the context of this paper, morphology refers to the sizes and shapes of particles. Reports of such investigations can be found in some references, where factors affecting the precipitation behaviour such as temperature, pH, rate of addition of reagents are varied and the consequent change in morphology are monitored by various automated techniques [32, 33].

However, none of the above mentioned have worked on actual industrial UOCs or report the morphology of these samples. This task is also made more challenging due to the presence of impurities that can influence the morphology as well as the lack of complete information regarding production processes.

In addition to the applicability of Raman spectroscopy, in this paper, the feasibility of studying the morphology of some UOCs using scanning electron microscopy (SEM) and image analysis are also explored and discussed. SEM has the added advantage of allowing direct observations of size and shape simultaneously compared to other automated techniques such as particle size analyser based on diffraction, sedimentation etc. It is also readily available in the nuclear forensics laboratory since it is necessary to study the physical appearance as well as to obtain chemical composition of unknown material, with the help of energy dispersive spectrometry.

Finally, with the eventual goal of assessing the strengths and limitations of Raman spectroscopy and morphological parameters as signatures for nuclear forensics, *principal component analysis (PCA)* is used to provide an overview of the data. Observations of clusters, patterns, trends or outliers often results from the analysis. PCA also reveals relationships between the observations and the variables and among the variables themselves. PCA does it by finding new relationships between variables and presenting them differently without modifying the data. In so doing, the number of variables needed to present the data is also drastically reduced [34].

2. Experimental

2.1. Investigated material

A total of 89 industrial UOC samples from various mining/milling facilities in the world were analyzed using Raman spectrometer as summarized in chapter 2.2. These UOCs have different compositions such as ammonium diuranate (ADU), sodium diuranate (SDU), uranyl peroxide (UO_4), uranyl hydroxide (UH) or $UO_2(OH)_2$, ammonium uranyl carbonate (AUC), UO_3 or U_3O_8. Six samples of AUC, ADU, SDU, UO_4 and $UO_2(OH)_2$ were synthesized in our laboratory [35]. All powder samples were pressed into pellet using a hydraulic press that made handling of the sample easier and this also reduced the risk of contamination. In addition, a nuclear grade UO_2 fuel pellet was also measured.

17 industrial UOC samples were randomly selected for morphological assessment. Tiny amount of powder were placed in a mortar crusher and grinded in analytical grade ethanol. The gentle grinding is aimed to disintegrate large agglomerates. A small portion of the sample solution was pipetted onto aluminium disk holder with membrane filter. All samples were coated with 10 nm Au to increase conductivity.

2.2. Instrumentation

2.2.1. Raman spectrometers

A bench-top model of Raman spectrometer known as Senterra from Brukers® (available in the Institute for Nuclear Waste Disposal, Karlsruhe, Germany) was mainly used in this study. All 95 samples were analysed using Senterra while selected samples were analysed with two other Raman spectrometers. One of them is a hand-held spectrometer, FirstDefender|RM from Ahura Scientific®

(from IAEA) and the other, a laboratory spectrometer, T64000 from HORIBA Jobin Yvon® (available in Institute for Transuranium Elements).

2.2.2. Infrared spectrometer

Fourier Transform Infrared (FT-IR) measurements were performed using Perkin Elmer System 2000 spectrometer from Perkin Elmer Ltd, Beaconsfield, UK), the details can be found elsewhere [22].

2.2.3. Scanning Electron Microscopy and Image Analysis

SEM of the model VEGA-TESCAN from Oxford instruments was used for taking images. For most samples, 2-5 images of 2560x2320 µm were acquired and the Image-Pro Analyzer 3D software v. 7.0 (Media Cybernetics, Inc., USA) with a pre-recorder macro was used to carry out the image analysis resulting in an output of 30 parameters describing shapes and sizes of the particles. A total of 65 images from 17 samples were analysed.

2.3. Data evaluation software

A PLS Toolbox version 7.5.2 (Eigenvectors Research, Inc., USA) for Matlab version 8.1 (The Matworks Inc, Natick, MA, USA) software was used for the multi-variate data analysis (PCA). Various pre-processing methods were used for Raman data (baseline correction, normalize, smoothing) and for image analysis (autoscale).

3. Results and Discussions

3.1. Raman spectroscopy

3.1.1. Spectral interpretation

Fig. 2 shows examples of the Raman spectra taken from four industrial UOCs with the hand-held device. In general, the spectrum is divided into three regions as these vibrations have different origins. Region I (900-250 cm^{-1}) containing the most intense peak(s) is due to symmetric stretch of UO_2^{2+}, known to be in the region of 750-900 cm^{-1} [36]. The small peaks found in region II (1200-900 cm^{-1}) have been attributed to process related impurities (which were verified by comparison with laboratory synthesized yellow cake) by spiking with the impurities in question [35]. These anionic impurities are often sulphates, nitrates and carbonates that are used in mining/milling processes. The observation and identification of such impurities in UOCs using Raman spectroscopy were firstly reported by us. Region III (2500-1200 cm^{-1}) has been associated with non-Raman effects and was in fact observed as electronic transitions with the use of different wavelength lasers. The full details can be found in reference [35].

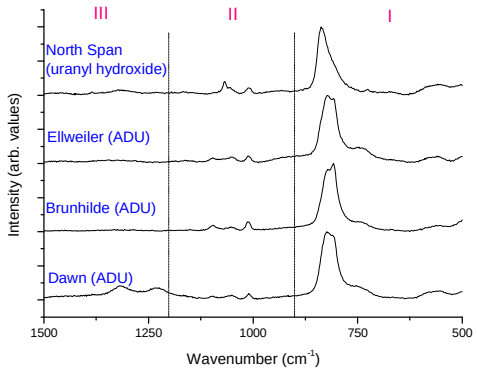

Fig. 2: Raman spectra of four industrial UOCs obtained by hand-held Raman spectrometer

3.1.2. Comparison of figure of merits in the analysis of UOCs by three dispersive spectrometers

It is pertinent to note that most of these UOCs fluoresce when higher frequency lasers such as 514.5 or 532 nm are used. Often, cracks and burnt marks could be observed after measurements and good quality spectra were difficult to obtain. Near-infrared laser, or red laser (785, 752.5 and 647.1 nm) sufficed in producing good quality spectra although at the expense of sensitivity, since Raman signals are proportional to ν^4 where ν is frequency. Figures of merit such as sensitivity and signal-to-noise ratio (defined according to [37]) and the detection capabilities of the three spectrometers are briefly featured in this paper. Table 1 denotes the overall performance in measuring five different UOCs, UO_2 powder and a nuclear grade UO_2 fuel pellet. The latter was analysed so that it could be compared to the UO_2 powder.

There are immediately a few observations from Table I that shall be summarized here. In general, Senterra and T64000 can analyse all the UOCs as well as UO_2 powder and pellet. However, hand-held Raman cannot measure dark powder such as UO_2 and U_3O_8 due to preferential absorption of light and poor reflective surfaces on a macroscopic scale. This is in contrast to the fuel pellet where a signal was picked up, thus highlighting the importance of surface optical properties in such an instance. These dark powdered samples (due to calcinations) could still be measured by Senterra and T64000, but with two orders of magnitude lower in intensity compared to other uncalcined UOCs. This also affects the detection of trace level impurities in such samples by Raman spectroscopy with more details found in reference [37].

Table I. Comparison of sensitivity, signal to noise ratio and the ability to detect characteristic bands and impurities present in measured compounds among the three spectrometers [37]. Calculated values were further normalised within each figure of merit for better readability.

		Type of compound						
Figures of merit		Ammonium diuranate	Sodium diuranate	UO_2 powder	UO_2 pellet	U_3O_8	Uranyl hydroxide	Uranyl peroxide
Sensitivity	*Portable*[1]	17.5	18.6	-	1.2	-	19.3	22.3
	Senterra[2]	36.8	***100.0***	0.3	2.4	0.4	16.8	45.3
	T64000[3]	1.9	3.4	0.007	0.04	0.03	0.3	0.2
Signal-to-noise ratio	*Portable*	31.2	24.6	-	10.9	-	15.5	12.8
	Senterra	47.3	***100.0***	2.7	19.2	4.8	59.4	31.9
	T64000	56.4	28.4	0.9	2.8	1.6	8.0	23.7
Detection capability (based on characteristic bands)	*Portable*	√	√	X	√	X	√	√
	Senterra	√	√	√	√	√	√	√
	T64000	√	√	√	√	√	√	√
Ability to detect impurities[4]	*Portable*	√	MP	NA	NA	X	√	MP
	Senterra	√	MP	NA	NA	X	√	MP
	T64000	√	MP	NA	NA	X	√	MP

MP: Most probable; NA: Not applicable (impurities were not observed)

[a] 785nm
[2] 785nm
[3] 752.5nm/647.1nm
[4] If present at ppm levels

3.1.3. Library database in hand-held Raman spectrometer

Given that the hand-held Raman spectrometer is equipped with an existing and customizable library, more than 40 spectra of measurable UOCs and the spectra of fuel pellet were stored in the spectrometer. This is a huge advantage of deploying Raman spectrometer as it allows real-time identification of unknown substances on top of its simple operation. The samples were tested as 'unknowns' to verify the matching accuracy of the detection algorithms. The details of this study can be found in a separate proceeding [38].

3.1.4. PCA analysis of Raman spectra

As seen in Fig. 3A (full circles), clusters or groups with similar composition such as UO_4, U_3O_8, SDU, UF_4 and AUC could be observed. However, UOCs such as ADU and UH (dotted circles) were found to overlap with each other. The corresponding loading plot is shown in Fig. 3B. Three principal components (PCs) could explain 75 % of the variance in the dataset. The clustering of supposedly different composition of ADU and UH is addressed in the following section with the use of infrared data to complement the Raman data.

3.2. Infrared spectroscopy

It is known that infrared spectroscopy based on absorption is generally more sensitive technique than Raman spectroscopy (scattering is 10^{10} times less probable than absorption) [39]. The data taken by FTIR for the same UOCs had been measured and the results were published [22]. Therefore, it is logical to use IR as a basis of comparison to verify the composition of UOCs. Fig. 4 depicts two pairs of industrial samples and laboratory synthesized ADU and UH. It is evident that given the observations of N-H bands (~3150 cm^{-1} and ~1400 cm^{-1}) of ADU (samples El Dorado, Delft, ADU) in IR, these supposedly Raman active bands [40] are not observed (data not shown here) due to a weaker response of near IR lasers (785 nm) and charge-coupled device (CCD) detectors. The use of lower laser wavelength (532 nm) with higher sensitivity, was unfortunately too energetic to be used for these UOC samples [37].

In addition, the Raman bands of North Span (ADU) and Delft (UH), El Dorado (ADU) and Alligator (UH) samples are highly similar within the pair. This explains why the clusters of ADU and UH (Fig. 3) are overlapping. On the other hand, the IR spectra of the respective pairs are rather different from each other and the ratios of the O-H/N-H bands of both ADUs are completely different from each other. From the qualitative perspective, the varying ratios of O-H/N-H bands could suggest that the compositions of ADUs are varied. Therefore, a sample classified as ADU (such as Delft) could be in fact a mixed UOC, both an ADU and uranyl hydroxide. It is very often the case where the uranium solution is often adjusted to an optimum pH with NH_3, NaOH, lime or MgO before its subsequent precipitation [9]. Using a two-step precipitation, application of lime in the first step is also a way to precipitate impurities [41]. Therefore, it is not unusual for these UOCs to have more than one composition. This is further supported by the IR of pure ADU and uranyl hydroxide (Fig. 5) synthesized in the laboratory by the precipitation of concentrated uranium nitrate solutions with ammonium hydroxide and magnesia respectively without the pre-adjustment of pH [35]. These findings would be investigated further especially in an attempt to verify the true composition of the UOCs.

3.3. Morphological assessment

It is known that the morphology of the final products such as U_3O_8 or UO_2 is influenced by the morphology of initial product such as uncalcined UOC [42].

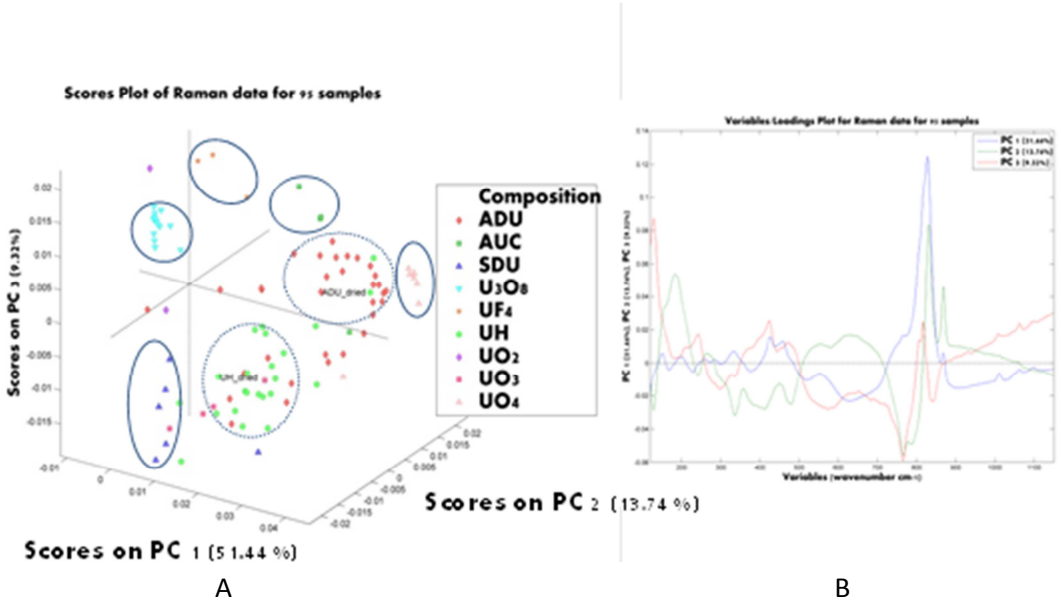

Fig. 3: A-Score plot revealing clusters of compounds among 95 spectra (95 samples); B- Loading plot of variables

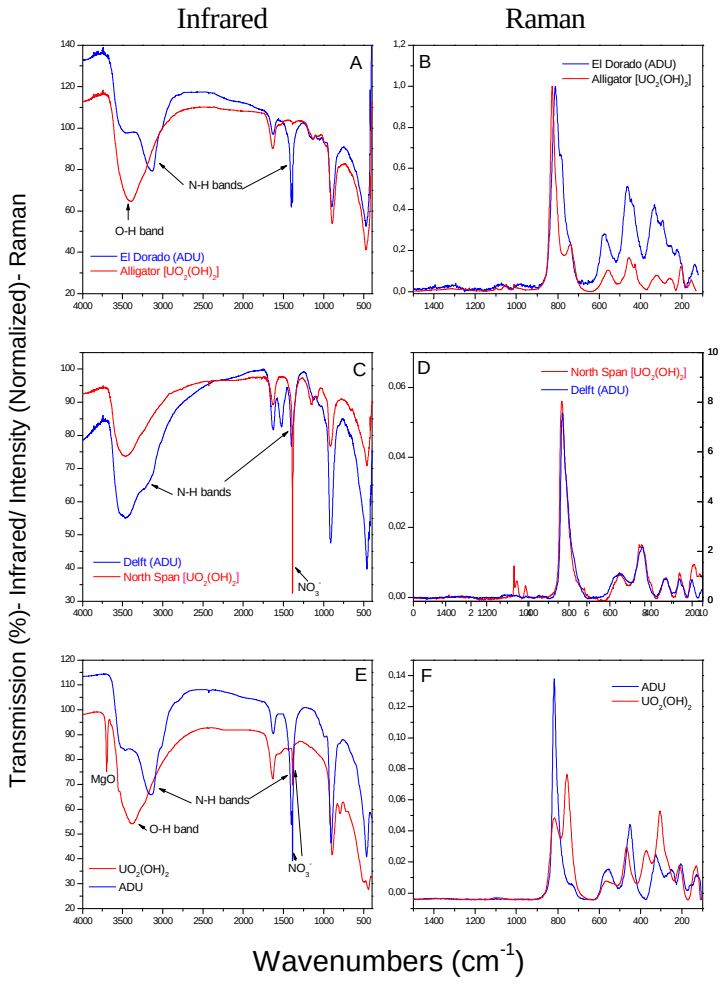

Fig. 4: IR and Raman of El Dorado and Alligator samples (A & B); IR and Raman of Delft and North Span samples (C & D); IR and Raman of laboratory synthesized ADU and $UO_2(OH)_2$ samples (E & F)

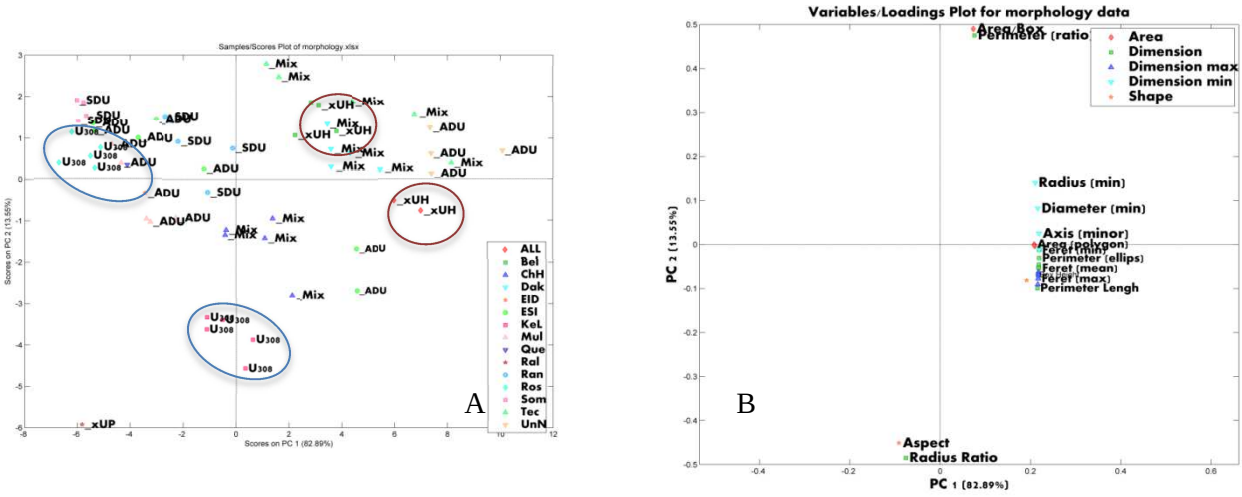

Fig. 5: A- Morphology analysis: Score plot of 15 samples; B- Loadings plot of variables

If this observation is true, it means that morphological parameters can be a potential signature for origin attribution. At the very least, in the scenario of an unknown UOC being analysed, for example, U_3O_8, its composition can be readily determined by rapid techniques like IR and/ or Raman spectroscopy and subsequently, its morphological parameters assessed complementarily for origin assessment.

Fig. 5 depicts the preliminary PCA graphs of 15 UOC samples (initial graph of 17 samples are not shown) after removing the outliers corresponding to the samples having big variances in the morphology characteristics from the others. There were in total, 30 parameters that were put into the data and subsequently 3 variables were removed to improve the data. Contrary to the observation of clusters among the compounds with similar composition for Raman data (Fig. 3), PCA of morphological data has the opposite effect. Each point on Fig 5A corresponds to a single image taken from the same preparation. As it can be observed, the points are located fairly close to each other with certainly some spread as well. In addition, it can be observed that two pairs of separate clusters of U_3O_8 and uranyl hydroxides from Key Lake/Rössing and Alligator/Belgian Congo respectively are located far from each other and this appeared to arise from different morphologies. It can also be observed that the use of 2 PCs could already explain 96 % of the variance in the dataset. The loading plot (Fig. 5B) reveals the relationship between 27 parameters (not all are visible) that are related to shape and shape of the particles. The above results are preliminary and needs to be tested with more samples and the repeatability/ reproducibility further assessed. However, it does demonstrate that the method of dispersing UOCs in this study, for SEM analysis appears to work.

4. Conclusions

It has been demonstrated that Raman spectroscopy is a useful tool for the measurement of UOCs despite the challenges of fluorescence and weaker Raman effects in comparison to IR. Impurities related to production processes were observed and identified and the exploitation of the complementary nature of both IR and Raman has led to considerable doubts of the true composition of ADUs/uranyl hydroxides especially for samples with mixed composition. This combination would be highly useful in the event of analysing unknown UOC. Raman spectrometers in the form of hand-held, bench-top and laboratory settings were compared, evaluated and the findings added values to the understanding of the differences in measuring different uranium compounds. Preliminary results of morphological data provide a promising outlook as a possible signature for origin assessment.

REFERENCES

[1] MAYER, K., M. WALLENIUS, and I. RAY, *Nuclear forensics- a methodology providing clues on the origin of illicitly trafficked nuclear materials.* Analyst 130 (2005) 433-441.

[2] WALLENIUS, M., K. MAYER, and I. RAY, *Nuclear forensic investigations: Two case studies.* Forensic Science International 156 (2006) 55-62.

[3] MAYER, K., M. WALLENIUS, and T. FANGHÄNEL, *Nuclear forensic science-From cradle to maturity.* Journal of Alloys and Compounds 444-445 (2007) 50-56.

[4] WALLENIUS, M., et al., *Nuclear forensic investigations with a focus on plutonium.* Journal of Alloys and Compounds, 444-445 (2007) 57-62.

[5] VARGA, Z., et al., *Analysis of uranium ore concentrates for origin assessment.* Proc. Radiochim. Acta 1 (2011) 1-4.

[6] BUDINGER, P.A., et al., *The Case of the Great Yellow Cake Caper.* Analytical Chemistry 52 (1980) 942A-948A.

[7] KEEGAN, E., et al., *Nuclear forensic analysis of an unknown uranium ore concentrate sample seized in a criminal investigation in Australia.* Forensic Science International 240 (2014)111-121.

[8] HAUSEN, D.M., *Characterizing and classifying uranium yellow cakes: A background.* JOM 50 (1998) 45-47.

[9] PREEZ, J.G.H.d., *A review of the industrial processes involving uranium- from the ore to the reactor.* Radiation Protection Dosimetry 26 (1989) 7-13.

[10] KEEGAN, E., et al., *The provenance of Australian uranium ore concentrates by elemental and isotopic analysis.* Applied Geochemistry 23 (2008) 765-777.

[11] BRENNECKA, G.A., et al., *Natural variations in uranium isotope ratios of uranium ore concentrates: Understanding the 238U/235U fractionation mechanism.* Earth and Planetary Science Letters 291 (2010) 228-233.

[12] VARGA, Z., et al., *Alternative method for the production date determination of impure uranium ore concentrate samples.* Journal of Radioanalytical and Nuclear Chemistry 290 (2011) 485-492.

[13] ŠVEDKAUSKAITE-LEGORE, J., et al., *Investigation of the isotopic composition of lead and of trace elements concentrations in natural uranium materials as a signature in nuclear forensics*, in *Radiochimica Acta* 95 (2007) 601-605.

[14] VARGA, Z., et al., *Application of Lead and Strontium Isotope Ratio Measurements for the Origin Assessment of Uranium Ore Concentrates.* Analytical Chemistry 81 (2009) 8327-8334.

[15] ŠVEDKAUSKAITĖ-LEGORE, J., et al., *Investigation of the sample characteristics needed for the determination of the origin of uranium-bearing materials.* Journal of Radioanalytical and Nuclear Chemistry 278 (2008) 201-209.

[16] HAN, S.H. et al., *Measurement of the sulphur isotope ratio ($^{34}S/^{32}S$) in uranium ore concentrates (yellow cakes) for origin assessment.* Journal of Analytical Atomic Spectrometry 28 (2013) 1919-1925.

[17] VARGA, Z., et al., *Determination of rare-earth elements in uranium-bearing materials by inductively coupled plasma mass spectrometry.* Talanta 80 (2010) 1744-1749.

[18] VARGA, Z., M. WALLENIUS, and K. MAYER, *Origin assessment of uranium ore concentrates based on their rare-earth elemental impurity pattern*, Radiochimica Acta 98 (2010) 771-778.

[19] KEEGAN, E., et al., *Attribution of uranium ore concentrates using elemental and anionic data.* Applied Geochemistry 27 (2012) 600-1609.

[20] KENNEDY, A.K., et al., *Non-volatile organic analysis of uranium ore concentrates.* Journal of Radioanalytical and Nuclear Chemistry 296 (2013) 817-821.

[21] BADAUT, V., M. WALLENIUS, and K. MAYER, *Anion analysis in uranium ore concentrates by ion chromatography.* Journal of Radioanalytical and Nuclear Chemistry 280 (2009) 57-61.

[22] VARGA, Z., et al., *Characterization and classification of uranium ore concentrates (yellow cakes) using infrared spectrometry.* Radiochim. Acta 99 (2011) 1-7.

[23] KLUNDER, G.L., et al., *Application of Visible/Near-Infrared Reflectance Spectroscopy to Uranium Ore Concentrates for Nuclear Forensic Analysis and Attribution.* Applied Spectroscopy 67 (2013) 1049-1056.

[24] PLAUE, J.W., et al., *Near infrared reflectance spectroscopy as a process signature in uranium oxides.* Journal of Radioanalytical and Nuclear Chemistry 296 (2013) 551-555.

[25] SIRVEN, J.-B., et al., *Towards the determination of the geographical origin of yellow cake samples by laser-induced breakdown spectroscopy and chemometrics.* Journal of Analytical Atomic Spectrometry 24 (2009) 451-459.

[26] LAUWERS, D., et al., *Characterisation of a portable Raman spectrometer for in situ analysis of art objects.* Spectrochimica Acta Part A: Molecular and Biomolecular Spectroscopy 118 (2014) 294-301.

[27] COLOMBAN, P., *The on-site/remote Raman analysis with mobile instruments: a review of drawbacks and success in cultural heritage studies and other associated fields.* Journal of Raman Spectroscopy 43 (2012) 1529-1535.

[28] IZAKE, E.L., *Forensic and homeland security applications of modern portable Raman spectroscopy.* Forensic Science International 202 (2010) 1-8.

[29] VÍTEK, P., et al., *Evaluation of portable Raman spectrometer with 1064nm excitation for geological and forensic applications.* Spectrochimica Acta Part A: Molecular and Biomolecular Spectroscopy 86 (2012) 320-327.

[30] MOGILEVSKY, G., et al., *Raman Spectroscopy for Homeland Security Applications.* International Journal of Spectroscopy 2012 (2012) 1-12.

[31] SIEBERT, F. and P. HILDEBRANDT, *Theory of Infrared Absorption and Raman Spectroscopy*, in *Vibrational Spectroscopy in Life Science*, Wiley-VCH Verlag GmbH &

Co. KGaA (2008) 11-16.

[32] KIM, K.-W., et al., *Effects of the different conditions of uranyl and hydrogen peroxide solutions on the behavior of the uranium peroxide precipitation.* Journal of Hazardous Materials 193 (2011) 52-58.

[33] RAJAGOPAL, S., T.P.S. ASARI, and C.S.P. IYER, *Particle size analysis of ammonium uranate prepared by conventional and homogenous methods of precipitation and their corresponding oxides.* Journal of Nuclear Materials 227 (1996) 300-303.

[34] ERIKSSON, L., et al., *Multi- and Megavariate Data Analysis: Principles and Applications*. (2001) Umetrics Academy.

[35] HO, D.M.L., et al., *Applicability of Raman Spectroscopy as a Tool in Nuclear Forensics for Analysis of Uranium Ore Concentrates.* Radiochimica Acta 101 (2013) 779-784.

[36] ČEJKA, J., et al., *Raman spectroscopic study of the uranyl carbonate mineral čejkaite and its comparison with synthetic trigonal* $Na_4[UO_2(CO_3)_3]$. Journal of Raman Spectroscopy 41 (2010) 459-464.

[37] HO, D.M.L., et al., *The use of different dispersive Raman spectrometers for the analysis of uranium compounds.* Vibrational Spectroscopy 73 (2014) 102-110.

[38] BERLIZOV, A., et al. *Assessing Capabilities of Handheld Raman Spectrometer FirstDefender RM for Complementary Access Applications*. in *Esarda 35th Annual Meeting*. (2013) Gruges, Belgium: European Safeguards Research and Development Association.

[39] MCCREERY, R.L., *Raman Spectroscopy for Chemical Analysis*, ed. J.N. Winefordner. 2000, Canada: John Wiley and Sons, Inc

[40] DEGEN, I.A. and G.A. NEWMAN, *Raman spectra of inorganic ions.* Spectrochimica Acta 49A (1993) 859-887.

[41] INTERNATIONAL ATOMIC EBERGY AGENCY, Uranium Extraction Technology, IAEA, Vienna (1993).

[42] CHOI, C.S., et al., *The influence of AUC powder characteristics on* UO_2 *pellets.* Journal of Nuclear Materials 153 (1988) 148-155.

143Nd/144Nd Ratio – A Powerful Signature for Origin Assessment of Natural Uranium Products

J. Krajko[a,b], Z. Varga[a], M. Wallenius[a], K. Mayer[a]

[a] European Commission
Joint Research Centre, Institute for Transuranium Elements
P.O Box 2340, 76125
Karlsruhe, Germany

[b] Delft University of Technology
Faculty of Applied Sciences
Mekelweg 15, 2629 JB
Delft, Netherlands

Abstract. Expanding the pattern of characteristic properties which helps to identify the origin of uranium-bearing sized material is one of the most important directions of nuclear forensic research and development. In this paper the usefulness of stable isotopic variations of Nd for provenance assessment in nuclear forensics has been evaluated. A novel procedure has been developed for the measurement of REE pattern, the $^{143}Nd/^{144}Nd$ isotope ratio and the Nd/Sm ratio in various uranium-bearing materials, such as uranium ores, and uranium ore concentrates (UOC). The method was validated by the measurement of standard reference materials (Morille, La Jolla, JB2 and BCR-2). The applicability of the method was demonstrated by the determination of $^{143}Nd/^{144}Nd$ isotope ratio in uranium samples originating from different uranium mines and milling facilities.

1. Introduction

Since the early 1990s illegal possession, transfer and other unauthorised acts involving nuclear materials have taken place. In order to identify the hazard, intended use and origin of the illicitly trafficked nuclear materials, new analytical methods using techniques such as radiometry, mass spectrometry and electron microscopy have been developed for nuclear forensics during the following years. Among the characteristic parameters that can be determined by the above-mentioned methods the concentration and the isotopic composition of some of the impurities of uranium materials have been found highly indicative to the feed material, production facility and its location as well as to the last chemical processing date of the nuclear material.

Up to now the isotopic patterns of Pb, Sr, and U have been investigated. Also the elemental pattern of the rare-earth elements (REE) has been studied and found characteristic to the geological formation of the uranium deposit [1-6]. Due to the similarity in chemical properties, their relative abundances remain mainly unaltered through the processing in the front-end of the nuclear fuel cycle. Among the REE, the $^{143}Nd/^{144}Nd$ isotope ratio is widely used in geology with ε notation and the $^{147}Sm/^{143}Nd$ isotope ratio for chronometry and provenance measurements. The $^{143}Nd/^{144}Nd$ ratio varies in nature due to the ^{147}Sm decay to ^{143}Nd ($T_{1/2}=1.06 * 10^{11}$ a). As ^{144}Nd is neither radioactive nor radiogenic, the number of ^{144}Nd atoms does not change with time, which makes it suitable as a reference isotope [7, 8]. Together with the other above-mentioned characteristic parameters in uranium, the Nd isotope ratio can be a promising signature for nuclear forensics. The measurement of $^{143}Nd/^{144}Nd$ isotope ratio in uranium samples is however analytically a challenging task as the concentration of Nd is very low

(<ppb level) due to the effective production and purification process. Therefore pre-concentration of REE, before the measurement by ICP-MS, is often required.

The present work aims at evaluating the usefulness of stable isotopic variations of Nd for provenance assessment in nuclear forensics. For that purpose a novel procedure has been developed for the measurement of REE pattern, the $^{143}Nd/^{144}Nd$ isotope ratio and the Nd/Sm ratio in various uranium-bearing materials, such as uranium ores, and uranium ore concentrates (UOC). After the pre-concentration of REE from the uranium matrix, Nd and Sm were separated and further concentrated by extraction chromatography. REE were measured by high resolution inductively coupled plasma mass spectrometry (HR-ICP-MS) and the Nd isotope ratio was determined by multi collector inductively coupled plasma mass spectrometry (MC-ICP-MS). The method was validated by the measurement of standard reference materials (Morille, La Jolla, JB2 and BCR-2). When combining the REE pattern with the isotopic information of Nd, the deposit type where the uranium was mined from can be assessed with higher probability, therefore helping in the origin determination of unknown nuclear materials.

2. Experimental

2.1. Reagents

All labware was cleaned thoroughly with dilute ethanol, followed by dilute nitric acid, and finally rinsing with high purity water. For all the dilutions high-purity water was used (UHQ System, USF Elga, Germany). Hydrochloric and nitric acid was of Suprapur grade (Merck, Darmstadt, Germany), although the nitric acid was further purified by sub-boiling distillation.

Analytical grade $Fe(NO_3)_3$ salt was used as carrier for the co-precipitation (Alfa Aesar, Karlsruhe, Germany). Analytical grade sodium-hydroxide and ammonium-carbonate used for the precipitation were purchased from Sigma Aldrich (St Louis, MO, USA). Ammonium carbonate was further purified prior the use by $Fe(OH)_3$ precipitation in order to remove the trace-level lanthanide impurities. TRU™ and Ln™ extraction chromatographic resin (Triskem International, Bruz, France) was used for the lanthanide group separation and the forthcoming Nd separation. Respectively 1.6 mL and 0.4 mL of the resin was placed in plastic Bio-Rad holders and plugged with porous Teflon frit (Reichelt Chemietechnik Heidelberg, Germany) on the top of the resin to avoid mixing.

For the optimization of the chemical separation procedure and the measurements by ICP-MS, lanthanide standard solution and monoelemental Nd and Sm standard solutions (Alfa Aesar, Karlsruhe, Germany) were prepared by the dilution from 1000 μg mL^{-1}, and 100 μg mL^{-1} standard solutions, respectively. The Morille (Cetama, France) U_3O_8 certified reference material, was used for the validation of the co-precipitation method. The relative background (signal to noise ratio) was less than 2% for all sample. All uncertainties quoted are given as expanded uncertainty using a coverage factor of k=2 with last significant digits in parenthesis.

2.2. Instrumentation

The analysis of REE fractions from the co-precipitation step was carried out using an ELEMENT2 (Thermo Electron Corp., Bremen, Germany) double-focusing magnetic sector inductively coupled plasma mass spectrometer (ICP-SFMS) in low resolution mode (R = 300).). Instrument optimisation with respect to maximum sensitivity low UO^+/U^+ ratio was carried out using 1 ng g^{-1} multielement solution (Merck, Darmstadt, Germany.

Nd isotope ratio measurements were performed with a NuPlasma™ (NU Instruments, Oxford, United Kingdom) double-focusing multi-collector inductively coupled plasma mass spectrometer (MC-ICP-MS) in low mass resolution mode. The sample introduction was done by a low-flow Teflon micro-concentric nebulizer in combination with a DSN-100 desolvation unit (NU Instruments, Oxford, United Kingdom). Instrument optimisation with respect to maximum sensitivity was carried out using

a 100 ng g^{-1} Nd monoelemental solution (Alfa Aesar, Karlsruhe, Germany). The sensitivity was approximately 500 mV for $^{143}Nd^{+}$ in 100 ng g^{-1} Nd standard solution.

The distribution of U and Th during the co-precipitation was followed by gamma spectrometric measurements using a well-type HPGe detector (Canberra Industries Inc., USA). The measured spectra were evaluated using Genie 2000 v2.1 software. All gamma spectrometric measurements were performed as relative measurements to the original starting material before and after the separation at fixed geometry. Measurement time varied between 600 and 5400 s.

2.3. Sample preparation

Approximately 0.5 g of samples were weighed into a Teflon Erlenmeyer and dissolved in 6 mL 8 M ultra-pure nitric acid while heating to 90 °C on a hot-plate for 12 hours covered with a PE stopcock. Aliquot of this stock solution, corresponding to about 10 mg uranium of sample, was weighed into a polyethylene vial and diluted using ultra-pure water in order to adjust the required HNO_3 concentration. The extraction chromatographic separation was performed in two stages.

(1) The lanthanide content of the sample aliquots was separated using extraction chromatography by the selective retention of trivalent lanthanides on the TRU™ resin in 3 M nitric acid medium.

(2) In the second step, Ln resin was used in 0.05 M HCl medium for the Nd separation from Sm, which interferes otherwise with the ICP-MS analysis. A method blank was processed through the entire dissolution and separation procedure parallel to the samples. The final Nd fractions were analysed by MC-ICP-MS [9, 10].

In case of samples with low Nd concentration (<50 ng/g) pre-concentration of the samples was performed before the above mentioned two step chromatographic separation in the following way: About 3.0 mL of the stock solutions were transferred into a 50 mL polyethylene centrifuge vials corresponding to about 200 mg of uranium. Ln, Th and U were precipitated as hydroxides (pH 12-14) with 40 % sodium hydroxide in the presence of 2 mg Fe(III) carrier. The supernatant, containing most of the alkali-soluble matrix elements (e.g. alkali metals) were carefully discarded after thorough centrifugation. Subsequently the precipitate was rinsed with high-purity water. Selective (re-)dissolution of uranium from the precipitate was done with 10 mL 1% $(NH_4)_2CO_3$ as uranium forms soluble di- and tri-carbonato complexes between pH 5-8 [11]. This step was repeated three to five times until clear solution was obtained; assuring that U was removed from the sample to the highest extent possible. The residual precipitate containing the Ln and Th was dissolved in 2 mL 3 M nitric acid to be in suitable form for further concentration by extraction chromatography.

3. Results and discussion

Representative aliquots of the supernatant of pre-concentration procedure were collected after each separation step in order to control uranium decontamination and Th recovery factors by gamma spectrometric measurements parallel to the separation. The achievable U decontamination factor was in the magnitude of $10^2 – 10^4$, sufficiently high to use the extraction chromatography afterwards. From this final solution, containing the Ln and Th, 100 µL aliquots were taken for mass spectrometric measurements to evaluate recoveries and decontamination factors. The method was validated by the measurement of reference material (Morille, Cetama), the recovery for the certified rare earth elements (Sm, Eu, Gd, Dy) was better than 90% [12].

Three UOC sample (Rabbit Lake, Mary Kathleen and Nabarlek) were analysed to compare the REE pattern with and without pre-concentration step in order to verify that no interferences were introduced to the samples by the used reagents. As one can see from the Figure 1 the normalised REE patterns agree well.

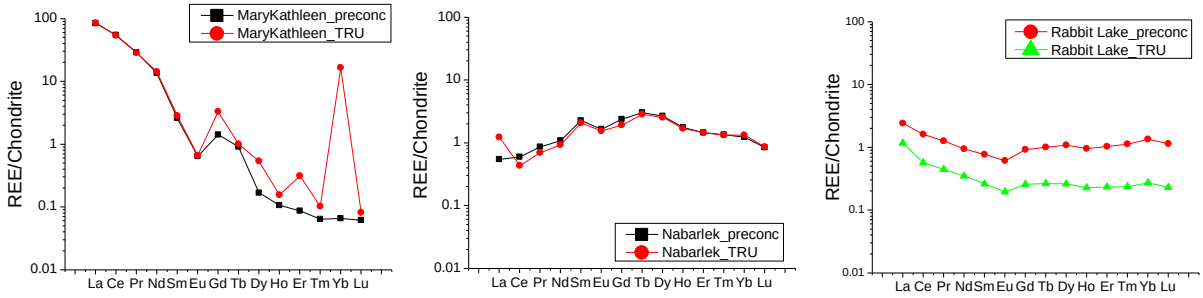

FIG 1 REE patterns of investigated uranium ore concentrate samples obtained from two separation type extraction chromatography (TRU) and co-precipitation (preconc)

Table 1 Measured $^{143}Nd/^{144}Nd$ isotope ratios in the investigated uranium ore concentrate samples. All uncertainties quoted are given as expanded uncertainty using a coverage factor of k=2 with last significant digits. $^{143}Nd/^{144}Nd_{TRU}$ corresponds to the results obtained by using only TRU separation, while $^{143}Nd/^{144}Nd_{preconc}$ are the results of the present method with preconcentration.

Sample	**Country**	**Deposit type**	**c_{Nd} (ng/g)**	**$^{143}Nd/^{144}Nd_{TRU}$**	**$^{143}Nd/^{144}Nd_{preconc}$**
ESI	Canada	Phosphate	90	<DL	0.51225(9)
Rössing	Namibia	Intrusive	15	0.51363(230)	0.51346(34)
Shirley Basin	USA	Sandstone	8	<DL	0.51356(61)

The $^{143}Nd/^{144}Nd$ isotope ratio of U-ore and UOC samples was measured and plotted against the Sm/Nd elemental ratio of the samples (Fig.2). The measured $^{143}Nd/^{144}Nd$ value of the BCR-2 standard was 0.512598(78). This value agrees with the certified value 0.512629(8) within uncertainty [13]. The Nd isotope ratio of Rössing sample had been measured previously using only EXC sequential separation and it resulted in a $^{143}Nd/^{144}Nd$ ratio of 0.51363(230). Comparing to our new result 0.51346(34), obtained with the improved sample pre-concentration procedure, one can see that the values are in good agreement. Moreover the uncertainty of the new result is almost an order of magnitude better. Shirley Basin (USA) and ESI (CAN) were previously under detection limit, but with the combined sample preparation procedure precise results were possible to obtain (Table 1).

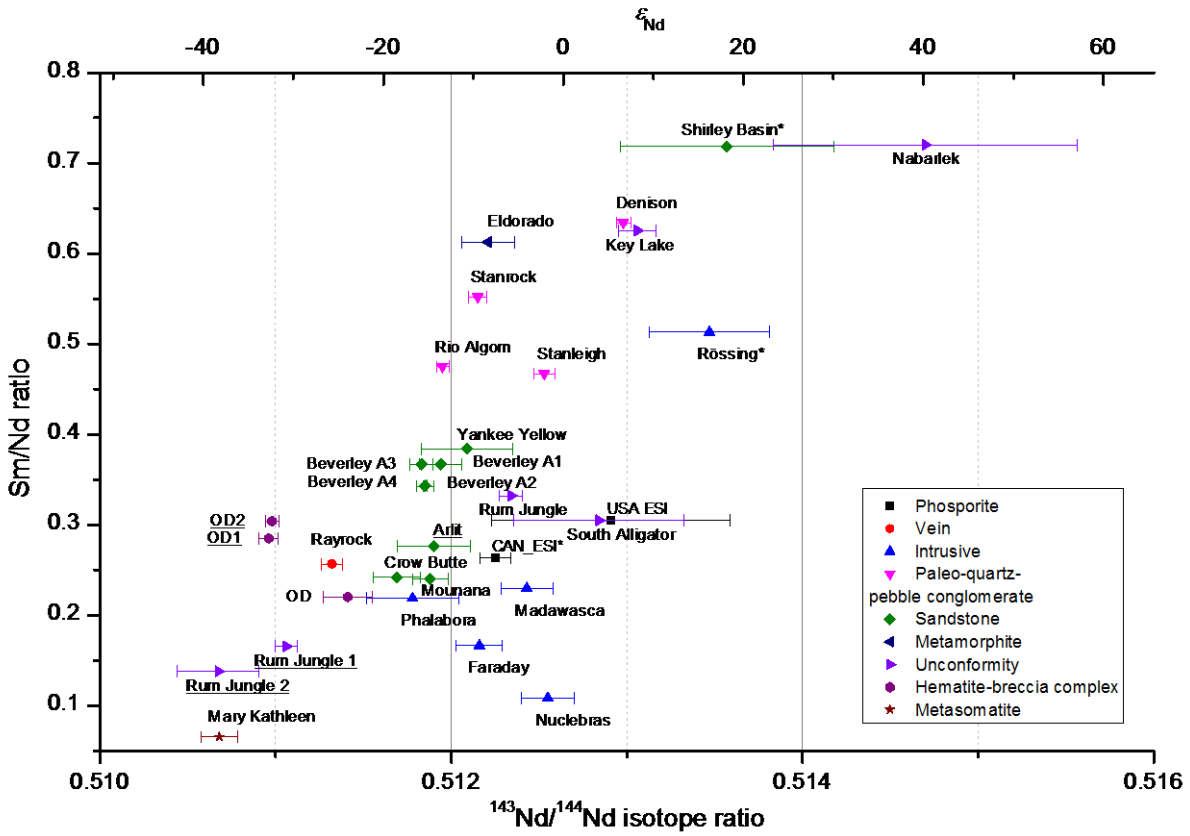

FIG 2 Variation of the $^{143}Nd/^{144}Nd$ ratio as a function of Sm/Nd ratio in the investigated uranium ore and uranium ore concentrate samples. 'OD' – Olympic Dam; 'underlined labels' correspond to ore samples, 'label with asterisk' correspond to samples prepared by combined separation procedure [10].

The obtained results show that the $^{143}Nd/^{144}Nd$ isotope ratio is highly variable in UOCs and ores; the value ranges between 0.510 and 0.515. This variation shows a relatively good correlation with the Sm/Nd ratio in the sample. This initial study suggests that certain deposit types (e.g. intrusive or quartz-pebble conglomerate) can have specific ε_{Nd} values, while for other deposit types we observe larger spread of the values. The $^{143}Nd/^{144}Nd$ isotope ratio in the investigated samples has also smaller within mine variation when comparing to other stable isotope ratios studied previously for nuclear forensic purposes, such as Pb and Sr. As the $^{143}Nd/^{144}Nd$ ratio is related to the Sm/Nd ratio in the ores, we can assume that this smaller within-mine variation derives from the fact that both the parent (^{147}Sm) and daughter (^{143}Nd) nuclides are rare-earth elements and have similar chemical properties, which means that their ratio is less affected during the history of the rock, e.g. by fractionation due to weathering. In contrast to the Sm/Nd ratio, the Sr and Pb isotope variation is due to the presence of the chemically highly different parent/daughter pairs (Rb/Sr and U/Pb), which are more prone to fractionation. The results are discussed detailed elsewhere [10].

Investigation of correlation of Nd isotope ratio variations with Sr isotope ratio has been started, as previous geological studies showed that reservoirs with high $^{143}Nd/^{144}Nd$ tend to have low $^{87}Sr/^{86}Sr$ ratios (Fig 3.). This trend could be explained by the hypothesis that Nd and Sr isotopic variations in the earth mantle are the results of magmatic process induced Sm/Nd and Rb/Sr fractionations [14]. However, we can see that such correlation is not that obvious in case of uranium ore concentrates and further studies need to be done to understand properly the correlation between Nd and Sr isotopic variations and the deposit types.

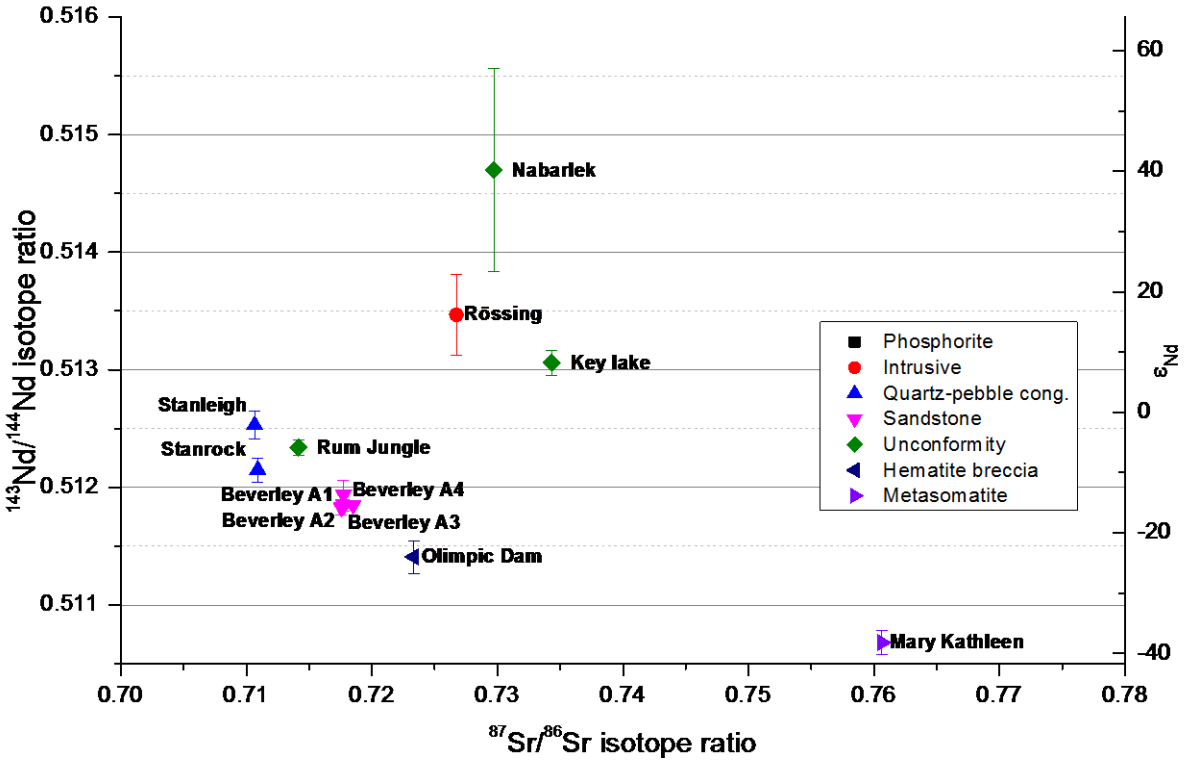

FIG 3 Distribution of $^{87}Sr/^{86}Sr$ isotope ratio as a function of $^{143}Nd/^{144}Nd$ ratio in the investigated uranium ore and uranium ore concentrate samples.

4. Conclusions

Novel procedure has been developed for the measurement of REE pattern, the $^{143}Nd/^{144}Nd$ isotope ratio and the Nd/Sm ratio in various uranium-bearing materials, such as uranium ores, and ore concentrates (UOC). The obtained results show that the $^{143}Nd/^{144}Nd$ isotope ratio is highly variable in UOCs and ores; the value ranging between 0.510 and 0.515. This variation shows a relatively good correlation with the Sm/Nd ratio in the sample. The $^{143}Nd/^{144}Nd$ isotope ratio in the investigated samples has also smaller within mine variation when comparing to other stable isotope ratios studied previously for nuclear forensic purposes. Although, the results show that certain deposit types have overlapping Nd isotope ratios and therefore it cannot be used as an exclusive signature, the $^{143}Nd/^{144}Nd$ isotope ratio is still useful when complemented with other characteristics of the materials. The data evaluation and interpretation to find a correlation between the determined Nd ratio and other isotopic variation (e.g. Sr, and Sm) and the deposit type is on-going. The presented method, however, is not just useful for trace-level Nd isotope ratio analysis as demonstrated, but it is also a versatile and straightforward sample preparation procedure, which can be applied to pre-concentrate and separate other elements of interest, such as Th, Pu or Am from a single sample aliquot. These are just few examples of the promising potential of the new developed pre-concentration procedure.

REFERENCES

[1] INTERNATIONAL ATOMIC ENERGY AGENCY, Nuclear Forensics Support, IAEA Nuclear Security Series No. 2, IAEA, Vienna (2006).

[2] PAYO, L., et al. Investigation of the oxygen isotopic composition in oxidic uranium compounds as a new property in nuclear forensic science. Fresenius' J. Anal. Chem. **371** (2011) 348–352.

[3] HAN, S.H., et al., Measurement of the sulphur isotope ratio (34S/32S) in uranium ore concentrates (yellow cakes) for origin assessment, J. Anal. At. Spectrom. **28** 12 (2013) 1919.

[4] VARGA, Z., et al., Application of lead and strontium isotope ratio measurements for the origin assessment of uranium ore concentrates. Anal. Chem. **81** (2009) 8327–34.

[5] SRNCIK, M., et al., Investigation of the ^{236}U/ ^{238}U isotope abundance ratio in uranium ores and yellow cake samples. Radiochim. Acta **99** (2011) 335–339.

[6] RICHTER, S., et al., Isotopic "fingerprints" for natural uranium ore samples. Int. J. Mass Spectrom. **193** (1999) 9–14.

[7] NIE, J., et al., Integrated provenance analysis of a convergent retroarc foreland system: U–Pb ages, heavy minerals, Nd isotopes, and sandstone compositions of the Middle Magdalena Valley basin, northern Andes, Colombia. Earth-Sci. Rev. **110** (2012) 111–126.

[8] MAAS, R., et al., Sm-Nd isotope systematics in uranium-rare earth element mineralization at the Mary Kathleen uranium mine, Queensland. Econ Geol **82** (1987) 1805–1826.

[9] VARGA, Z., et al., Determination of rare-earth elements in uranium-bearing materials by inductively coupled plasma mass spectrometry. Talanta **80** (2010) 1744–1749.

[10] KRAJKO, J., et al., Application of Neodymium Isotope Ratio Measurements for the Origin Assessment of Uranium Ore Concentrates. Talanta, (2014) DOI: 10.1016/j.talanta.2014.06.022.

[11] GOVINDAN, P., et al., Ammonium uranyl carbonate (AUC) based process of simultaneous partitioning and reconversion for uranium and plutonium in fast breeder reactors (FBRs) fuel reprocessing. J. Radioanal. Nucl. Chem. **295** (2013) 77–82.

[12] KRAJKO, J., et al., Determination of trace-levels of Lanthanides and Thorium samples. European Winter Conference on Plasma Spectrochemistry, Krakow, Poland, (2013).

[13] RACZEK, I., et al., Neodymium and Strontium Isotope Data for USGS Reference Materials BCR-1, BCR-2, BHVO-1, BHVO-2, AGV-1, AGV-2, GSP-1, GSP-2 and Eight MPI-DING Reference Glasses. Geostand Geoanalytical Res. **27** (2003) 173.

[14] DEPAOLO, D. J., Neodymium Isotope Geochemistry: An Introduction. Minerals and Rocks Series no. 20. Springer-Verlag, ISBN 3 540 18648 4. (1988).

Measurement of Sulphur Isotopic Ratio for the Nuclear Forensic Investigation of Uranium Ore Concentrates (Yellow Cakes)

Z. Varga[a], S-H. Han[a,b], J. Krajko[a], M. Wallenius[a], K. Song[b], K. Mayer[a]

[a] European Commission
Joint Research Centre, Institute for Transuranium Elements
P.O Box 2340, 76125
Karlsruhe, Germany

[b] Korea Atomic Energy Research Institute
Daejeon, 305-353
Republic of Korea

Abstract. A novel method has been developed for the measurement of the $n(^{34}S)/n(^{32}S)$ isotope ratio in uranium ore concentrate (yellow cake) samples for the origin assessment in nuclear forensics. The leachable sulphate is separated and pre-concentrated by anion exchange separation followed by the $n(^{34}S)/n(^{32}S)$ ratio measurement using multi-collector inductively coupled plasma mass spectrometry. The method was validated by the measurement of standard reference materials (IAEA-S-2, IAEA-S-3 and IAEA-S-4) and the $\delta^{34}S$ value could be determined with an expanded uncertainty between 0.45‰ and 1.9‰ expressed with a coverage factor of 2. The method was then applied for the analysis of uranium ore concentrates of world-wide origin. In the studied materials distinct $n(^{34}S)/n(^{32}S)$isotope ratios could be observed, which can be a promising signature for the nuclear forensic investigations to identify the source of unknown nuclear materials. By the investigation of the sulphur isotope ratio variation during UOC production from ore to U_3O_8 product it was shown that process reagents have radical effect on the $n(^{34}S)/n(^{32}S)$, thus the sulphur isotope ratio is in most cases a process-related signature.

1. Introduction

As an answer to the illicit trafficking of nuclear materials in the 1990s a new scientific topic has emerged, commonly referred to now as *nuclear forensics* [1]. The aim of the nuclear forensic investigations is to identify the hazard and origin of the confiscated or found nuclear materials and ultimately strengthen security measures and prevent nuclear terrorism thereafter. Over the last few years several signatures of nuclear materials have been investigated and developed to establish the links between the measurable parameters of the unknown material in question and the source of the nuclear materials. These measurable parameters or signatures include e.g. elemental or anionic impurities, isotopic composition, structural analysis, morphology and age determination [1-6]. This complex dataset can give information about the source of uranium ore or feed materials, process and the production facility.

Among the other signatures the natural sulphur isotope variation also gives a possibility to discriminate samples of different origin. The sulphur isotope abundance shows relatively high variation in nature due to the large relative mass difference between its isotopes, the variety of chemical forms and the widespread occurrences in nature [7].

The sulphur variation is generally expressed as the amount ratio of $n(^{34}S)/n(^{32}S)$ of the two principal sulphur isotopes relative to the IAEA V-CDT (Vienna Cañon Diablo Troilite meteorite) standard in parts per thousand (permil, ‰) [8]. The $\delta^{34}S$ values of samples relative to the V-CDT scale in ‰ are calculated using the following equation:

$$\delta^{34}S_{V-CDT}(‰) = \left[\frac{\left(\frac{^{34}S}{^{32}S}\right)_{sample}}{\left(\frac{^{34}S}{^{32}S}\right)_{V-CDT}} - 1 \right] \times 1000 \quad (1)$$

where $(^{34}S/^{32}S)_{sample}$ and $(^{34}S/^{32}S)_{V\text{-}CDT}$ are the $n(^{34}S)/n(^{32}S)$ of ratio of sample and IAEA V-CDT standard, respectively. The $(^{34}S/^{32}S)_{V\text{-}CDT}$ is defined as 0.0441626 ± 0.0000078 (k = 2) [9, 10].

Typically, natural materials with oxidized sulphur have $\delta^{34}S$ values between +5 ‰ and +25 ‰, while for materials with reduced sulphur it ranges between -5 ‰ and +15 ‰ [11]. The sulphur isotope ratio in uranium ore deposits is also reported to exhibit large variation, such as in the sandstone-type uranium deposits of the Colorado Plateau and Wyoming (-20.5 to -17.8 ‰) or in the uranium roll-type deposit in South Texas, USA (-25 to -40 ‰). However, as the sulphur content in the nuclear material derives not only from the feedstock (ore), but is also introduced into the process stream as process chemical (e.g. as H_2SO_4 with an approximate $\delta^{34}S$ value of -5 to +15 ‰), its contribution to the final $\delta^{34}S$ value in the product has to be considered. Therefore, it is expected that sulphur isotopic composition can be indicative both for the process (chemicals used) and the ore type depending on the hydrometallurgical production route.

In order to investigate if the sulphur isotopic composition is a meaningful signature in nuclear forensics, a novel method has been developed and validated for the measurement of $n(^{34}S)/n(^{32}S)$ isotope ratio in uranium ore concentrates (yellow cakes) [11]. The developed ion exchange separation method effectively separates and pre-concentrates sulphate from uranium and the possibly interfering matrix components, such as cations. The measurement was performed by multi-collector inductively coupled plasma mass spectrometry. The applicability of the sulphur isotope ratio as a possible signature for nuclear forensics was tested by the measurement of several UOCs of world-wide origin, and also its variation was investigated during the UOC production from uranium ore to U_3O_8.

2. Experimental

2.1. Instrumentation

A NuPlasma™ (NU Instruments, Oxford, United Kingdom) double-focusing multi-collector inductively coupled mass spectrometer (MC-ICP-MS), equipped with 11 Faraday collectors and 3 discrete dynode electrode multipliers was used for the sulphur isotope ratio measurements. The instrument was operated at low mass resolution mode (R = 300). The samples were introduced into the plasma using a low-flow Teflon microconcentric nebulizer operated in a self-aspirating mode in combination with a desolvation unit (DSN-100, NU Instruments, Oxford, United Kingdom).

The anion (sulphate) measurements were performed by ion chromatography (Advanced Compact IC 861, Metrohm, Switzerland). The ion chromatograph is equipped with a chemical suppressor (Module MSM II) and a conductivity detector. The separation of sulphate was carried out using an anion exchange column (METROSEP A supp 5, 150 × 4.0 mm I.D.) preceded with a guard column (METROSEP Anion Dual 1, 50 × 4.6 mm I.D.).

2.2. Reagents and materials

For dilutions ultra-pure water was used (UHQ System, USF Elga, Germany). Suprapur grade nitric acid (Merck, Darmstadt, Germany) was used for the sample preparation. All other reagents used were of analytical grade. To prevent anionic contamination during the measurement, all lab ware was washed three times with ultra-pure water, dried in a laminar flow bench and stored in clean zipped bags. New and cleaned labware was used for each sample.

To validate the developed method, sulphur isotope ratio certified reference materials purchased from the International Atomic Energy Agency (IAEA) were used. For the analysis approximately 80 mg of the IAEA standards (S-1, S-2, S-3, S-4) were weighed into a screw-cap Teflon vial and dissolved in 5 mL of nitric acid while heating to 95 °C on a hotplate for 6 hours. After cooling to room temperature, sulphate concentrations in these stock solutions were measured by ion chromatography (IC). These stock solutions were subsequently diluted to 2 μg mL^{-1} (expressed as sulphur) in 1% HNO_3 for the sulphur isotope ratio measurement.

A total of 18 uranium ore concentrates originating from different mines were included in this study. The chemical compositions of the investigated uranium ore concentrates vary depending on the milling process applied in the different facilities. The samples investigated for the variation of sulphur isotope ratio variation during UOC production were obtained from an undisclosed UOC production facility. There the UOC production is carried out in the following five stages:

(a) Sulphuric acid leaching of the uranium ore
(b) Ion exchange separation
(c) Solvent extraction
(d) ADU precipitation using ammonia
(e) Calcination to U_3O_8

One production batch was followed during the UOC production, and samples were taken from the various stages. The sampled materials are assumed to be representative of the investigated single UOC production batch.

2.3. Separation of sulphate by ion exchange

100 – 300 mg of sample depending on the sulphur concentration was taken and 10 mL ultra-pure water was added in pre-cleaned plastic bottle. The samples were leached for 24 hours at room temperature and filtered with pre-rinsed 0.45 μm cellulose acetate syringe filters (Nalgene, USA) before the ion exchange separation.

For the separation of SO_4^{2-} from the leaching solution anion exchange resin (AG 1-X4, Cl^- form, 100 – 200 mesh, Bio-Rad Laboratories, USA) was applied. New column was used for every sample to avoid the risk of cross-contamination. For the column preparation, 1 mL of the resin was placed in a poly-prep column (0.8 x 4 cm, Bio-Rad Laboratories, USA) and porous polyethylene frit (120 μm pore size, Reichelt Chemietechnik Heidelberg, Germany) was placed on the top to avoid mixing. Before use, the resin was converted into nitrate form by elution with 10 mL of 3 M HNO3 and pre-conditioned with 10 mL of 0.03 M HNO_3. The flow rate for the resin column was about 0.6-0.7 mL min^{-1}. Before loading, the resin was conditioned again with 10 mL of 0.03 M HNO_3. After loading, the resin was washed with 10 mL of 0.03 M HNO_3 and subsequently SO_4^{2-} was eluted using 3 mL of 0.3 M HNO_3. An aliquot was taken for the recovery measurement of SO_4^{2-} by ion chromatography. Further details can be found elsewhere [11].

2.4. Measurement of $^{34}S/^{32}S$ by MC-ICP-MS

During the sulphur isotope ratio ICP-MS analysis dominantly two types of isobaric interferences need to be taken into account to achieve accurate results: doubly charged metals ions (e.g. $^{64}Ni^{2+}$, $^{64}Zn^{2+}$ or $^{68}Zn^{2+}$) and oxide/hydrate molecular ions (e.g. $^{16}O_2^+$, $^{1}H^{16}O_2^+$ or $^{16}O^{18}O^+$). Doubly charged isobaric interferences can be efficiently removed by using a prior chemical separation by the ion exchange process. On the other hand, the significant interferences by oxygen and hydrogen containing polyatomic ions cannot be eliminated using only chemical separation. In our method the oxide and hydrate species were eliminated by the application of a desolvation system. The background intensities for 1% HNO_3 solution at m/z = 32 and m/z = 34 were about 0.2 V and 0.006 V, respectively. In comparison, the intensities of 2 μg mL^{-1} S standard were 4 V and 0.19 V at m/z = 32 and m/z = 34, respectively. The contribution of blank for a 2 μg mL^{-1} S solution is estimated to be approximately 5%. As the blank intensity and the instrumental mass discrimination can change during the measurement sequence, a blank1–standard–blank2–sample bracketing procedure was used for the measurements. To correct for mass discrimination, the IAEA-S-1 standard was used, and 1% HNO_3 solution was used for background correction. The sulphur concentration of the standards and samples for the MC-ICP-MS measurement was adjusted to approximately 2 μg mL^{-1} by dilution with 1% HNO_3. For the IAEA-S-4 and the separated uranium samples, Ag standard solution was added to obtain a final Ag concentration of 27 μg mL^{-1} (equivalent to 4:1 molar ratio of Ag^+/SO_4^{2-}). It was found that sulphur can be lost via the applied desolvation system coupled to the MC-ICP-MS, which can be overcome by adding Ag^+ to the measured sample. This approach also provides matching the sample to the bracketing standard, thus assures accurate results [11].

2.5. Data evaluation

The measured raw intensities were corrected for the background using the preceding blank sample. Then the obtained net $^{34}S/^{32}S$ isotope ratio of the sample was corrected for the instrumental mass discrimination using the bracketing IAEA-S-1 standard (external standardisation). For the correction the $^{34}S/^{32}S$ isotope abundance ratio of the IAEA-S-1 is 0.0441493 ± 0.0000080 (k = 2) used [8]. Finally, the $\delta^{34}S$ values related to the V-CDT scale were calculated using Equation (1). Three replicates were measured for each sample. For the estimation of the measurement uncertainty the ISO GUM (Guide to the Expression of Uncertainty in Measurements) approach was adapted. The calculation was performed with the GUM Workbench software. The model developed was based on Equation (1), taking into account the uncertainty contributions from the measured $n(^{34}S)/n(^{32}S)$ isotope ratios of the IAEA-S-1 bracketing standard and the sample, the isotope abundance ratio of the IAEA-S-1 (0.0441493 ± 0.0000080, k = 2), and the uncertainty of the assigned V-CDT $\delta^{34}S$ value (0.0441626 ± 0.0000078, k = 2) [8]. All uncertainties are reported as expanded uncertainties (U) with a coverage factor k = 2.

3. Results and discussion

3.1. The $n(^{34}S)/n(^{32}S)$ ratio in nuclear materials

The developed method was applied for the measurement of uranium ore concentrates. The $n(^{34}S)/n(^{32}S)$ results are collected in Table I and shown in Figure 1 together with the sulphate concentrations measured by ion chromatography [11]. Clear differences in the $\delta^{34}S$ values of the uranium ore concentrates can be observed. As the $\delta^{34}S$ value differs in several cases from the reported average $\delta^{34}S$ value of sulphuric acid (-5 to +15 ‰), it suggests that the sulphur content of the uranium ore can significantly contribute to the sulphur content of the final product, thus the measured $\delta^{34}S$ value is indicative of the uranium ore. Since the $\delta^{34}S$ values of several samples from different origin overlap, the sulphur isotopic composition can be used only as a comparative signature for the origin assessment, i.e. to use the parameter to verify or exclude of an assumed (declared) origin of a nuclear material by the measurement of a comparison sample. Moreover, in a few cases the $v^{34}S$ values can indicate a predictive nature: the El Mesquite, Crow Butte and US Mobile samples are milled by in-situ leaching from sandstone-type deposit using carbonate lixiviant, followed by ion exchange separation.

As sulphuric acid is not used in these processes in high amount compared to other metallurgical processes (e.g. acidic leaching with H_2SO_4, or use of H_2SO_4 for the solvent extraction purification), and the sulphide minerals associated with sandstone-type uranium have significantly low $\delta^{34}S$ values, we can assume that the low $\delta^{34}S$ value together with the low sulphate content can be a useful predictive signature for uranium ore concentrates produced by in-situ leaching from sedimentary sandstone-type deposits, which are one of the major sources for uranium production (approximately 18% of world uranium resources).

Table I. $\delta^{34}S_{VCDT}$(‰) values for various uranium ore concentrate samples (n = 2). Uncertainties are expressed as expanded uncertainties with a coverage factor of 2

Uranium ore concentrate sample	$\delta^{34}S$(‰)	SO_4^{2-} concentration (μg/g)
Gunnar (Canada)	16.3 ± 1.4	2136
Rabbit Lake (Canada)	14.9 ± 2.0	3529
Madawaska (Canada)	2.3 ± 2.0	4958
Queensland (Australia)	-0.8 ± 1.2	5150
Olympic Dam (Australia)	16.0 ± 1.2	43206
Stanrock (Canada)	1.1 ± 1.1	47780
El Mesquite (USA)	-15.4 ± 1.2	1268
US Mobile (USA)	-10.3 ± 1.2	230
Shirley Basin (USA)	4.2 ± 2.0	36530
Crow Butte (USA)	-12.3 ± 2.1	2115
Yeelirrie (Australia)	15.0 ± 1.5	4402
Dyno (Canada)	18.3 ± 2.0	1710
Eldorado (Canada)	0.8 ± 1.5	16445
Rössing (Namibia)	10.4 ± 0.9	4675
Palabora (South Africa)	7.2 ± 1.6	410
Arlit (Niger)	12.5 ± 1.7	190
McArthur River (Canada)	8.6 ± 1.1	20053
Mounana (Gabon)	11.0 ± 0.9	11793

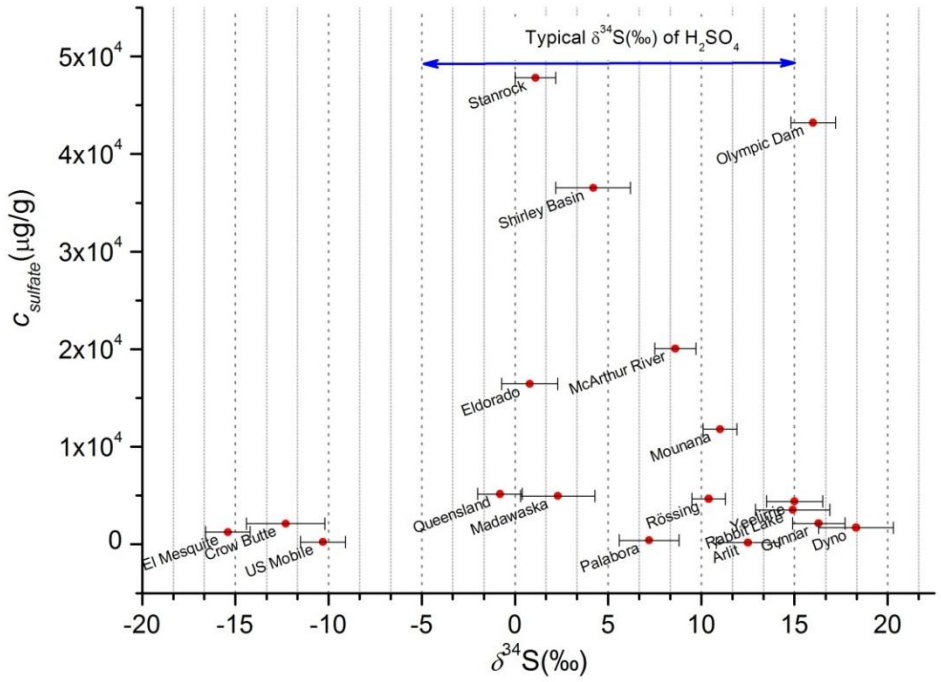

FIG. 1. Distribution of $\delta^{34}S_{VCDT}$(‰) and sulphate concentration of the analysed uranium ore concentrates. The relative combined standard uncertainty of the sulphate determination by ion chromatography is less than 10%.

3.2. Variation of n(^{34}S)/n(^{32}S) ratio in UOC production

The developed method was applied for the measurement of intermediate products in the course of a uranium ore concentrate production. In the undisclosed facility UOC is produced in the following way: in the first stage the uranium ore is leached with sulphuric acid, then the leachate is purified by ion exchange, then solvent extraction. Uranium is precipitated using ammonia, the resulted ammonium uranate (AU) is calcined to U_3O_8 as the final product. The material flow was sampled at each stage, the sulphur concentration and the $n(^{34}S)/n(^{32}S)$ was measured with the method described before.

The sulphur concentrations and $n(^{34}S)/n(^{32}S)$ results are shown in Fig. 2. Knowing that sulphur is added in high amount to the process flow in various forms (e.g. as H_2SO_4 for leaching and ion exchange elution or as Na_2SO_4 solution during solvent extraction for back-extraction) it is obvious that the sulphur contribution from process reagents is high. The sulphur concentration of the investigated samples is significantly higher at the ion exchange and solvent extraction stages (second and third stage, respectively) than in the ore leachate (first stage) (Fig. 2), which means that the contribution of sulphur from the process chemicals is increasing. After the solvent extraction purification the sulphur as impurity is gradually removed during the AU precipitation and calcination. In these stages the $n(^{34}S)/n(^{32}S)$ does not change, since no reagents with high sulphur content is added to the material process flow.

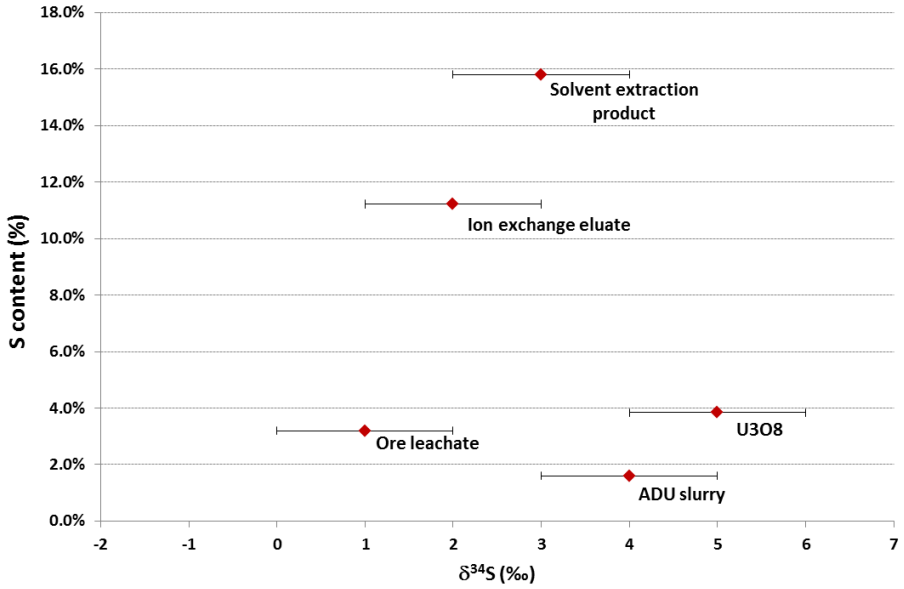

FIG. 2. Distribution of $\delta^{34}S_{VCDT}$(‰) and sulphate concentration of the samples during a uranium ore concentrate production.

4. Conclusions

A novel method has been developed and validated for the measurement of $n(^{34}S)/n(^{32}S)$ isotope ratio in uranium ore concentrates (yellow cakes). The ion exchange separation method effectively separates and pre-concentrates sulphate from uranium and the possibly interfering matrix components, such as cations. Determination of $n(^{34}S)/n(^{32}S)$ ratio in uranium ore concentrates of world-wide origin showed significant differences between the samples. This variation can be exploited to differentiate samples of different origin, for instance to verify or exclude a declared origin. Moreover, as the $n(^{34}S)/n(^{32}S)$ ratio can be indicative of the feed ore used for the production in several instances, the uranium ore deposit type can be identified, which can make this signature highly valuable to provide clues on the provenance of unknown nuclear materials, and thus trace them back to their source. Further studies are on-going to reveal further correlations between the $\delta^{34}S$ value in the ore concentrate and the deposit type (geolocation), to investigate the variation of $n(^{34}S)/n(^{32}S)$ ratio during the UOC production and the effect of process reagent on the $n(^{34}S)/n(^{32}S)$ value.

REFERENCES

[1] MAYER, K., et al., Nuclear forensic science: Correlating measurable material parameters to the history of nuclear material, Chem. Rev. **113** (2013) 884.

[2] MAYER, K., et al., Nuclear forensics - a methodology providing clues on the origin of illicitly trafficked nuclear materials, Analyst, **130** (2005) 433.

[3] VARGA, Z., et al., Analysis of Uranium Ore Concentrates for Origin Assessment, Radiochim. Acta **1** (2011) 1.

[4] KEEGAN, E., et al., Attribution of uranium ore concentrates using elemental and anionic data, Appl. Geochem. **27** (2012) 1600.

[5] SCHWANTES, J.M., et al., Nuclear archeology in a bottle: Evidence of pre-trinity U.S. weapons activities from a waste burial site, Anal. Chem. **81** (2009) 1297-1306.

[6] KRISTO, M.J., TUMEY, S.J., The state of nuclear forensics, Nucl. Instrum. Meth. Phys. Res. B **294** (2013) 656.

[7] THODE, H.G., Sulphur Isotopes in Nature and the Environment: An Overview, in: H.R. Krouse, V.A. Grinenko (Eds.) Stable Isotopes in the Assessment of Natural and Anthropogenic Sulphur in the Environment, John Wiley & Sons, New York (1991).

[8] DING, T., et al., Calibrated sulfur isotope abundance ratios three IAEA sulfur isotope reference materials and V-CDT with a reassessment of the atomic weight of sulfur, Geochim. Cosmochim. Acta **65** 15 (2001) 2433.

[9] DING, T., et al., Preparation of two synthetic isotope mixtures for the calibration of isotope amount ratio measurements of sulfur, International Journal of Mass Spectrometry, **197** 1-3 (2000) 131-137.

[10] COPLEN, T.B., et al., Isotope-abundance variations of selected elements (IUPAC technical report), Pure Appl. Chem. **74** 10 (2002) 1987.

[11] HAN, S.H., et al., Measurement of the sulphur isotope ratio (34S/32S) in uranium ore concentrates (yellow cakes) for origin assessment, J. Anal. At. Spectrom. **28** 12 (2013) 1919.